



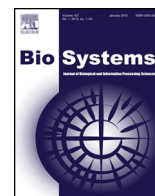
<b>Title</b>	Integrated signaling pathway and gene expression regulatory model to dissect dynamics of Escherichia coli challenged mammary epithelial cells
<b>Authors(s)</b>	den Breems, Nicoline Y., Nguyen, Lan K., Kulasiri, Don
<b>Publication date</b>	2014-10-05
<b>Publication information</b>	Breems, Nicoline Y. den, Lan K. Nguyen, and Don Kulasiri. "Integrated Signaling Pathway and Gene Expression Regulatory Model to Dissect Dynamics of Escherichia Coli Challenged Mammary Epithelial Cells." Elsevier, October 5, 2014. <a href="https://doi.org/10.1016/j.biosystems.2014.09.011">https://doi.org/10.1016/j.biosystems.2014.09.011</a> .
<b>Publisher</b>	Elsevier
<b>Item record/more information</b>	<a href="http://hdl.handle.net/10197/9791">http://hdl.handle.net/10197/9791</a>
<b>Publisher's statement</b>	This is the author's version of a work that was accepted for publication in Biosystems. Changes resulting from the publishing process, such as peer review, editing, corrections, structural formatting, and other quality control mechanisms may not be reflected in this document. Changes may have been made to this work since it was submitted for publication. A definitive version was subsequently published in Biosystems (126, (2014)) DOI:10.1016/j.biosystems.2014.09.011. Published under an Attribution-NonCommercial-NoDerivs 3.0 Unported (CC BY-NC-ND 3.0) license.
<b>Publisher's version (DOI)</b>	<a href="https://doi.org/10.1016/j.biosystems.2014.09.011">10.1016/j.biosystems.2014.09.011</a>

Downloaded 2026-05-02 01:13:06

The UCD community has made this article openly available. Please share how this access benefits you. Your story matters! (@ucd\_oa)



© Some rights reserved. For more information



# Integrated signaling pathway and gene expression regulatory model to dissect dynamics of *Escherichia coli* challenged mammary epithelial cells



Nicoline Y. den Breems<sup>a,b,\*</sup>, Lan K. Nguyen<sup>c</sup>, Don Kulasiri<sup>a</sup>

<sup>a</sup> C-fACS, Centre for Advanced Computational Solutions, Lincoln University, New Zealand

<sup>b</sup> Division of Cancer Research, University of Dundee, Dundee, United Kingdom

<sup>c</sup> Systems Biology Ireland, University College Dublin, Dublin 4, Ireland

## ARTICLE INFO

### Article history:

Received 7 August 2014

Received in revised form 25 September 2014

Accepted 28 September 2014

Available online 5 October 2014

### Keywords:

Integrated network

Signaling pathway

Gene regulatory network

ODE

NFκB

Mastitis

## ABSTRACT

Cells transform external stimuli, through the activation of signaling pathways, which in turn activate gene regulatory networks, in gene expression. As more omics data are generated from experiments, eliciting the integrated relationship between the external stimuli, the signaling process in the cell and the subsequent gene expression is a major challenge in systems biology. The complex system of non-linear dynamic protein interactions in signaling pathways and gene networks regulates gene expression.

The complexity and non-linear aspects have resulted in the study of the signaling pathway or the gene network regulation in isolation. However, this limits the analysis of the interaction between the two components and the identification of the source of the mechanism differentiating the gene expression profiles. Here, we present a study of a model of the combined signaling pathway and gene network to highlight the importance of integrated modeling.

Based on the experimental findings we developed a compartmental model and conducted several simulation experiments. The model simulates the mRNA expression of three different cytokines (*RANTES*, *IL8* and *TNFα*) regulated by the transcription factor NFκB in mammary epithelial cells challenged with *E. coli*. The analysis of the gene network regulation identifies a lack of robustness and therefore sensitivity for the transcription factor regulation. However, analysis of the integrated signaling and gene network regulation model reveals distinctly different underlying mechanisms in the signaling pathway responsible for the variation between the three cytokine's mRNA expression levels. Our key findings reveal the importance of integrating the signaling pathway and gene expression dynamics in modeling. Modeling infers valid research questions which need to be verified experimentally and can assist in the design of future biological experiments.

© 2014 The Authors. Published by Elsevier Ireland Ltd. This is an open access article under the CC BY-NC-ND license (<http://creativecommons.org/licenses/by-nc-nd/3.0/>).

## 1. Introduction

Gene expression is the result of the perturbation of a hierarchically organized and tightly controlled network of interacting elements in signaling pathways and gene regulation networks in the cell. These large number of interacting biochemical reactions show the emergent properties such as homeostasis and robustness with respect to perturbations (Ling et al., 2013). As more interactions between these signaling elements are identified,

it becomes clear that signaling does not necessarily occur through parallel, linearly independent processes (Hornberg et al., 2006). Interactions can occur at many hierarchical levels and signaling proteins can influence gene network regulation, which leads to complex behavior (Bhalla and Iyengar, 1999). To understand these properties we need to study the system rather than the individual components using computational, mathematical techniques and biological knowledge, a systems biology approach (Suresh Babu et al., 2006). Ordinary differential equations (ODEs) are the preferred technique for modeling the dynamics of quantitative and qualitative aspects of signaling pathways and gene network regulation over time (de Jong and Ropers, 2006).

External stimuli to cells activate signal transduction pathways to initiate transcription-factor (TF) driven gene expression in gene regulatory networks. Transcription factors are often pleiotropic and involved in gene expression profiles of multiple genes and

\* Corresponding author at: C-fACS, Centre for Advanced Computational Solutions, Lincoln University, Lincoln New Zealand, Tel.: +64 3 3252811.

E-mail addresses: [n.denbreems@dundee.ac.uk](mailto:n.denbreems@dundee.ac.uk), [aledni@gmail.com](mailto:aledni@gmail.com) (N.Y. den Breems), [lan.nguyen@ucd.ie](mailto:lan.nguyen@ucd.ie) (L.K. Nguyen), [Don.Kulasiri@lincoln.ac.nz](mailto:Don.Kulasiri@lincoln.ac.nz) (D. Kulasiri).

therefore multiple biological processes and phenotypes. Due to complexities involved in intertwined signaling processes, the mathematical studies of signaling pathways (e.g., Chen et al., 2009; Goldstein et al., 2004; Suresh Babu et al., 2006; Vera et al., 2008; Vera et al., 2007; Wolkenhauer et al., 2005) and gene regulatory pathways (e.g., Schlitt et al., 2007; Xie et al., 2007) are conducted separately even though these pathways often have interdependent interactions that significantly affect the inter- and intra-cellular functionalities. In several cases the gene expression is influenced by the dynamics of the translocation of the transcription factor to the nucleus (Hoffmann et al., 2002; Sillitoe et al., 2007). Altering the dynamics of the signaling pathway influences the gene network regulation and therefore the gene expression profile which result in altered protein production and phenotype. Therefore, understanding the interaction between the signaling and gene network regulation will improve our understanding of the gene expression profiles and the underlying dynamics.

Here, we integrate the modeling and analysis of the signaling pathway and gene regulatory network. We show that the origins of underlying dynamics differentiating the cytokine's gene expression following a perturbation can be found in the signaling pathway but not in the gene regulatory network. To this end, we use cytokine mRNA expression profiles in bovine mammary epithelial cells. Mammary epithelial cells invoke the immune response in mastitis. Mastitis is the result of an inflammatory event in the mammary gland usually caused by a variety of bacteria. Bovine mastitis is one of the major diseases in the dairy industry worldwide and causes distress for the animal (De Ketelaere et al., 2006). The economic impact leads to a worldwide cost of US \$25 billion per annum (Pareek et al., 2005). In humans, mastitis is associated with the increased transmission of bacterial infections (Wang et al., 2007) and human immunodeficiency virus (HIV) passing from mother to child (John et al., 2001).

### 1.1. Cytokine mRNA expressions in mammary epithelial cells

Gene expression studies of mammary epithelial cells identified pro-inflammatory cytokines such as *RANTES*, *IL8* and *TNF $\alpha$* , expressed at a higher level in mammary epithelial cells challenged by *Escherichia coli* (Griesbeck-Zilch et al., 2008; Lahouassa et al., 2007; Lutzow et al., 2008; Pareek et al., 2005; Tao et al., 2007). Previously, variations in mRNA expressions of the cytokines, such as *RANTES*, *IL8* and *TNF $\alpha$*  in mastitis have been reported (De Schepper et al., 2008; Griesbeck-Zilch et al., 2009; Rainard et al., 2006). The precise regulation of cytokine expression is essential for the regulation of the response to the infection. It is not completely understood how the cytokine expression is regulated.

### 1.2. Toll like receptor signaling

In mammary epithelial cells challenged with *E. coli* the toll like signaling activates the translocation of NF $\kappa$ B to the nucleus, which in turn initiates cytokine expression (Bannerman et al., 2004). Briefly, on the membrane of the epithelial cells, toll like receptors (TLR) recognizes the *E. coli* bacteria because of the molecular pattern, the endotoxin lipopolysaccharide (LPS) on the bacterial wall (Kawai and Akira, 2006) (Fig. 1).

TLRs are the primary line of defense against invading pathogens (Doyle and O'Neill, 2006) initiating the toll like receptor signaling (Petzl et al., 2008). Experimental studies by Werner et al. showed that *E. coli* bacteria, which engages TLR4, elicit a small increase in IKK activity in the first 30 min, followed by a larger increase between 45 and 90 min, attenuating in the late phase (Werner et al., 2005). This allows for stimulus specific signal processing of NF $\kappa$ B regulated genes such as the cytokines studied in this paper (Hoffmann et al., 2006; Werner et al., 2005). The TLR signaling

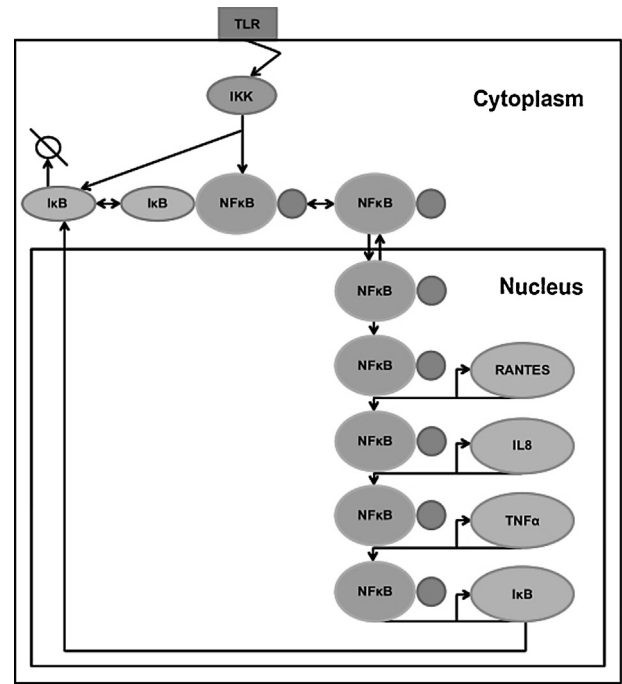


**Fig. 1.** Conceptual model of TLR- $\text{IKK}$ -NF $\kappa$ B signaling. The TLR receptor on the cell membrane recognizes the bacterial challenge. The signaling pathway activates the kinase IKK which breaks the  $\text{I}\kappa\text{B}$ -NF $\kappa$ B dimer. As a result, the transcription factor NF $\kappa$ B translocates to the nucleus initiating gene expression. Among the genes expressed are the  $\text{I}\kappa\text{B}$  isoforms ( $\text{I}\kappa\text{B}\alpha$ ,  $\text{I}\kappa\text{B}\beta$ ,  $\text{I}\kappa\text{B}\epsilon$ ) which bind with NF $\kappa$ B in the cytoplasm to prevent translocation of NF $\kappa$ B to the nucleus. This process creates a negative feedback loop for the translocation of NF $\kappa$ B to the nucleus. For clarity, only  $\text{I}\kappa\text{B}$  is shown in the picture representing three isoforms. In the model all three isoforms  $\text{I}\kappa\text{B}\alpha$ ,  $\text{I}\kappa\text{B}\beta$  and  $\text{I}\kappa\text{B}\epsilon$  are included as individual reactions. In addition the cytokines initiated by the transcription factor NF $\kappa$ B studied in this work, *RANTES*, *IL8* and *TNF $\alpha$* , are shown.

pathway therefore triggers gene expression initiating inflammatory and immune responses in the fight against *E. coli* infection (Akira et al., 2006) by activating the translocation of nuclear factor-kappa-B (NF $\kappa$ B) transcription factor to the nucleus (Strandberg et al., 2005) (Fig. 1). NF $\kappa$ B is a principal transcription factor in mammalian signaling (Cheong et al., 2008) and has been recognized as the 'master switch' in regulating the expression of various cytokines (Hayden et al., 2006). NF $\kappa$ B translocation does not require protein synthesis for its activation, allowing for fast reaction, within minutes, to inflammation (Hoffmann and Baltimore, 2006). The pattern and the timing of the translocation of NF $\kappa$ B to the nucleus lead to specific transcriptional outputs in NF $\kappa$ B regulated genes (Sillitoe et al., 2007).

### 1.3. NF $\kappa$ B signaling

In the cytoplasm NF $\kappa$ B is inactive as an  $\text{I}\kappa\text{B}$ -NF $\kappa$ B heterodimer (Fig. 1). NF $\kappa$ B activity is largely controlled by three  $\text{I}\kappa\text{B}$  isoforms,  $\text{I}\kappa\text{B}\alpha$ ,  $\text{I}\kappa\text{B}\beta$  and  $\text{I}\kappa\text{B}\epsilon$ , which bind to NF $\kappa$ B in the cytoplasm preventing transport of NF $\kappa$ B to the nucleus (Hoffmann et al., 2002). TLRs send signals to  $\text{I}\kappa\text{B}$  kinase (IKK) and IKK phosphorylates  $\text{I}\kappa\text{B}$ , which results in degradation of the  $\text{I}\kappa\text{B}$ -NF $\kappa$ B heterodimer and free NF $\kappa$ B. NF $\kappa$ B can then translocate to the nucleus and bind to DNA to function as a transcription factor for a large number of genes. In addition, NF $\kappa$ B initiates  $\text{I}\kappa\text{B}\alpha$  transcription, which therefore acts as a strong negative feedback loop in NF $\kappa$ B activity (Fig. 1). Negative feedback loops can provide stability, linearity, and influence the frequency response or change the response into step response simulating an on/off switch

(Brandman and Meyer, 2008).  $I\kappa B\epsilon$  is also induced by NF $\kappa$ B, with a delay relative to  $I\kappa B\alpha$ . The two feedback loops are in anti-phase and the role of  $I\kappa B\epsilon$  is to dampen  $I\kappa B\alpha$  mediated oscillations during long lasting NF $\kappa$ B activity (Kearns and Hoffmann, 2008).

Stability of the NF $\kappa$ B response is essential for the regulation of gene expression. Several diseases, including diabetics (Bragt et al., 2009) cancer and chronic inflammation (Fraser, 2008) have been related to the impairment of the NF $\kappa$ B regulation. In addition, immune responses such as inflammation, cell proliferation, apoptosis (Viatour et al., 2005) and milk protein levels (Connelly et al., 2010) are regulated by NF $\kappa$ B. NF $\kappa$ B levels as result of chronic mastitis were raised in milk (Boulanger et al., 2003). Targeted inhibition of NF $\kappa$ B signaling reduced milk loss and apoptotic signaling, which are of great concern during mastitis (Connelly et al., 2010). However, lack of regulation of the NF $\kappa$ B response can lead to severe diseases such as sepsis (Liew et al., 2005). Therefore, intricate knowledge of the NF $\kappa$ B regulation and the effect on the cytokine gene expression is of importance for the treatment and understanding of mastitis.

#### 1.4. Mathematical models

Several models using ODEs to simulate the TLR–IKK–NF $\kappa$ B signaling have been published (Covert et al., 2005; Hoffmann et al., 2002; Kearns et al., 2006; Lipniacki et al., 2004; Werner et al., 2005). These models have played a critical role in understanding the innate immune response aspects in TLR–IKK–NF $\kappa$ B signaling (Hoffmann and Baltimore, 2006) because the dynamics of biological networks are often difficult to identify with *in vivo* or *in vitro* experiments (Thakar et al., 2007). For example, some signaling pathways encode information not just as protein concentrations or location, but via temporal changes in the dynamics of those concentrations (Kell, 2005; Nelson et al., 2004). In these cases, an *in silico* model can provide additional insights into the dynamics of the network.

Sensitivity analysis can be used to analyze the role of signaling proteins, identify potential drug targets and plan future experiments. For instance, the *in silico* simulation of NF $\kappa$ B pathway dynamics as a result of inhibitor drugs indicated the potential for inhibition of upstream events with low drug concentrations (Sung et al., 2004). Total inhibition of proteins can be modeled with knockout simulations. Biological experiments cannot always simulate knockout due to lethality, cost and ethical considerations. *In silico* knock out simulations are therefore a good alternative to investigate the influence of specific model components.

Robustness analysis can simulate the effect of the change in bacterial load, e.g., as a result of milking, over time and investigate the effect on the cytokine expression levels. While mathematical models are informative, model development can be time consuming and costly. One way to reduce time and experimental cost is to use a modular approach, extending an existing model. Werner et al. combined the knowledge of the TLR–IKK–NF $\kappa$ B signaling models by Hoffmann et al. (2002) and Kearns et al. (2006) and demonstrated that experimental IKK activity profiles of *E. coli* infection can be used to explain the effect of the feedback regulation of the two out of phase feedback loops established by the three  $I\kappa B$  isoforms on the NF $\kappa$ B activity with an *in silico* model (Werner et al., 2005). The patterns and timing of the translocation of NF $\kappa$ B lead to different transcriptional outputs in NF $\kappa$ B regulated genes (Sillitoe et al., 2007) and different subsets of NF $\kappa$ B target genes are activated by the changes in the time-dependent kinetic profiles of NF $\kappa$ B signaling (Vanden Berghe et al., 2006). However, this model does not investigate the relationships between the mechanisms in the signaling pathway and the NF $\kappa$ B dynamics which result in the gene expression regulated by NF $\kappa$ B.

## 2. Objectives

The goal of this research is to demonstrate the necessity for integrated modeling of signaling and gene network regulation when studying cellular behaviors. We examine this paradigm with the analysis of an integrated model for the signaling pathway and gene regulatory network of mammary epithelial cells challenged by *E. coli*. To this end, we add a model of the gene network regulation of cytokine mRNA expression in mammary epithelial cells to the well-studied TLR–IKK–NF $\kappa$ B signaling pathway model developed by Werner et al. (2005). The developed model facilitates the investigation of the relationship between the signaling pathway variation and gene expression.

First, we discuss the model for the TLR–IKK–NF $\kappa$ B signaling pathway and incorporation of new ODEs accounting for the gene regulatory network for cytokine mRNA expression to form the integrated model, followed by the description of parameter estimation. Secondly, we perform sensitivity analysis and *in silico* knockout simulations to identify the mechanisms influencing the gene expression. Thirdly, we investigate the robustness of the gene network regulation, especially the influence of the variation of the transcription factor NF $\kappa$ B time profiles on the cytokine expression.

## 3. Model development and analysis

The need for an integrated model presented in this study is shown with the analyses of an integrated signaling and gene network regulation model of cytokine expression in primary bovine mammary epithelial cells challenged with LPS. The results are organized as follows: we develop the integrated model, and with the integrated model we perform sensitivity analysis and analyze *in silico* knockout models to show some of the mechanisms underlying the gene expression and the effect of possible drug targets. We then use robustness analysis to look at the effect of the perturbation of the model input, simulating a variation in bacterial load, on the cytokine expression.

### 3.1. Integrating the signaling pathway and gene regulation network

Based on the conceptual model as shown in Fig. 1, we developed the model for the TLR–IKK–NF $\kappa$ B signaling pathway and gene regulation network for cytokine expression. The activation of the TLR–IKK–NF $\kappa$ B signaling and the translocation of NF $\kappa$ B from the cytoplasm to the nucleus was modeled with 24 differential equations by Werner et al. (2005). The translocation of NF $\kappa$ B is the output of the signaling pathway and the input, the transcription factor, for the gene regulation network. In order to develop the combined model we extended the model with the gene regulation network. The gene network regulation is modeled with ODEs representing the mRNA expressions of *RANTES*, *IL8* and *TNF $\alpha$*  as a result of the translocation of the transcription factor NF $\kappa$ B into the nucleus.

The reactions in the model are formulated as uni-, bi- and tri-molecular processes according to the law of mass action. The model is divided in two compartments, cytoplasm and nucleus. Compartmentalization is achieved by representing a single protein as multiple species, one for each compartment. Protein transport is modeled as the movement of species between the compartments with first order kinetics making the process computationally tractable. The model input is represented with a piecewise linear function representing IKK stimulation (Fig. S3 in the Supplement) (Werner et al., 2005).

The concentration of cytokine mRNA can be described by the difference between the mRNA synthesis ( $rsr_x$ ) and degradation ( $d_{n_x}$ ) (Eqs. (1)–(6)).



$rsr_{xn}$  = NFκB induced mRNA synthesis rate.  $d_{nx}$  = mRNA degradation rate.  $h_{anx}$  = coefficient to represent transcriptional nonlinearity, such as cooperative binding and multiple transcription factors (with  $x$  replaced by  $r$  (*RANTES*),  $8$  (*IL8*) or  $TNF\alpha$  ( $TNF\alpha$ ) and  $n$  at the end of the species for nuclear NFκB (NFκBn), and  $t$  for mRNA, *IL8* mRNA (*IL8t*), *RANTES* mRNA (*RANtESt*), *TNFα* mRNA (*TNFαt*)).

In the model, we assume mRNA expression to be initiated by the transcription factor NFκB. It is known that multiple transcription factors are involved in the expression of the cytokines, but experimental data describing the multiple transcription factors are currently not available. We have modeled the action of the multiple transcription factors by modeling NFκB transcription factor for the initiation of the transcription of the cytokines with a coefficient of 3 to represent the other transcription factors involved similar to the signaling pathway model (Werner et al., 2005). In this model the function is modeled without the representation of saturation and can increase exponentially if no upper bound is defined. However the total concentration of NFκB is kept constant since no new NFκB is generated and the exponential increase of NFκB is therefore prevented (Werner et al., 2005).

The three differential equations (Eqs. (7)–(9)) representing *RANTES*, *IL8* and *TNFα* mRNA expression are added to complete the integrated model.

$$\frac{d[RANtES_t]}{dt} = +rsr_{rn} \times [NFkBn]^{h_{anr}} - rd_r \times [RANtES_t] \quad (7)$$

$$\frac{d[IL8_t]}{dt} = rsr_{8n} \times [NFkBn]^{h_{an8}} - rd_8 \times [IL8_t] \quad (8)$$

$$\frac{d[TNF\alpha_t]}{dt} = +rsr_{TNF\alpha n} \times [NFkBn]^{h_{anTNF\alpha}} - rd_{TNF\alpha} \times [TNF\alpha_t] \quad (9)$$

No residual transcription is modeled since *RANTES*, *IL8* and *TNFα* induction is dependent on the immune response. Parameters are estimated (Table 1) with the experimental data described in more detail in the Supplement Section S1.

The model allows us then to explore the influence of the dynamics of TLR–IKK–NFκB signaling and NFκB gene network regulation on the mRNA expression levels of the cytokines.

### 3.2. Gene network regulation parameter estimation

In Fig. 2, the model simulation with the estimated parameters are shown with the three experimental values (cells challenged with LPS from cow 1, cow 2, and cow 3, see Supplement

**Table 1**

Parameter values fitted in this study for the ordinary differential equations of cytokine mRNA expression.

Parameter	Value	Units	Description
$d_{nr}$	0.00039365	$\text{min}^{-1}$	Degradation <i>RANTES</i>
$rsr_{rn}$	5.28555	$\mu\text{M}^{-2}\text{min}^{-1}$	NFκB induced <i>RANTES</i>
$d_{n8}$	0.00175918	$\text{min}^{-1}$	mRNA synthesis Degradation <i>IL8</i>
$rsr_{8n}$	5.28555	$\mu\text{M}^{-2}\text{min}^{-1}$	NFκB induced <i>IL8</i> mRNA synthesis
$d_{nTNF\alpha}$	0.020602	$\text{min}^{-1}$	Degradation <i>TNFα</i>
$rsr_{TNF\alpha n}$	1.67	$\mu\text{M}^{-2}\text{min}^{-1}$	NFκB induced <i>TNFα</i> mRNA synthesis

Section S1 for a detailed description of the experiment). The input function is a piecewise linear function of IKK (Fig. S3 Supplement) representing the LPS challenge to the cells (Werner et al., 2005). There were no experimental data points at the time of the peak for the mRNA of *TNFα* or *IKκBα* (Fig. 2C and D), however, the model results were in line with experimental results previously described in the literature (Werner et al., 2005).

The parameter estimation is based on the experimental values of cells from cow 1. The general behavior of the mRNA expression is reproduced for the values of cow 2. The third data set (cow 3) indicates a lower expression level for *RANTES* and *IL8* than predicted by the model. Individual differences between cows can result in individual differences of cytokine expression levels and, as a result, mastitis resistance. Genetically determined differential expression levels of *RANTES* mRNA to pathogens between mastitis resistant and non resistant cows have been indicated earlier (Griesbeck-Zilch et al., 2009). The *RANTES* expression level difference between cows has been indicated as a selection option for mastitis resistant animals. However, the trend of the expression levels is the same and therefore the model can supply qualitative information on the underlying kinetics of the mRNA expression levels.

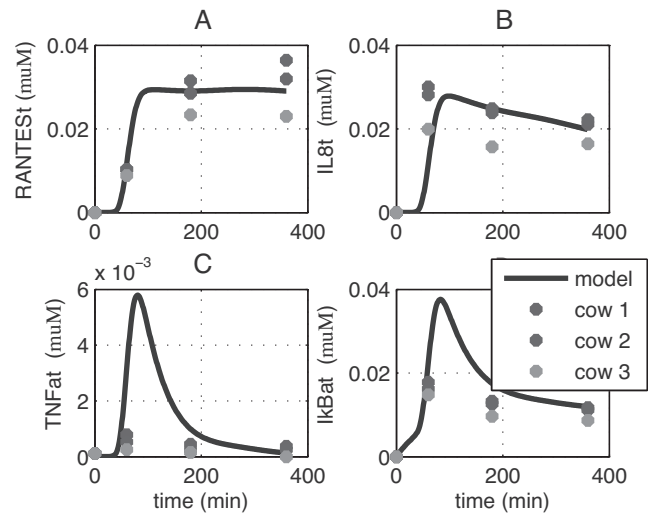


**Fig. 2.** Simulation of the model and experimental values. The outcome of the model predictions and the experimental values are shown for the samples of bovine epithelial cells from three cows (+, Δ, □). Estimation was performed with data from cow 1; the model was simulated for 360 min and the model predictions qualitatively compared with experimental data from cow 2 (Δ) and 3 (□). Solid lines represent the model outputs and (+) represent cow 1. The peaks were confirmed with experimental values in the literature.

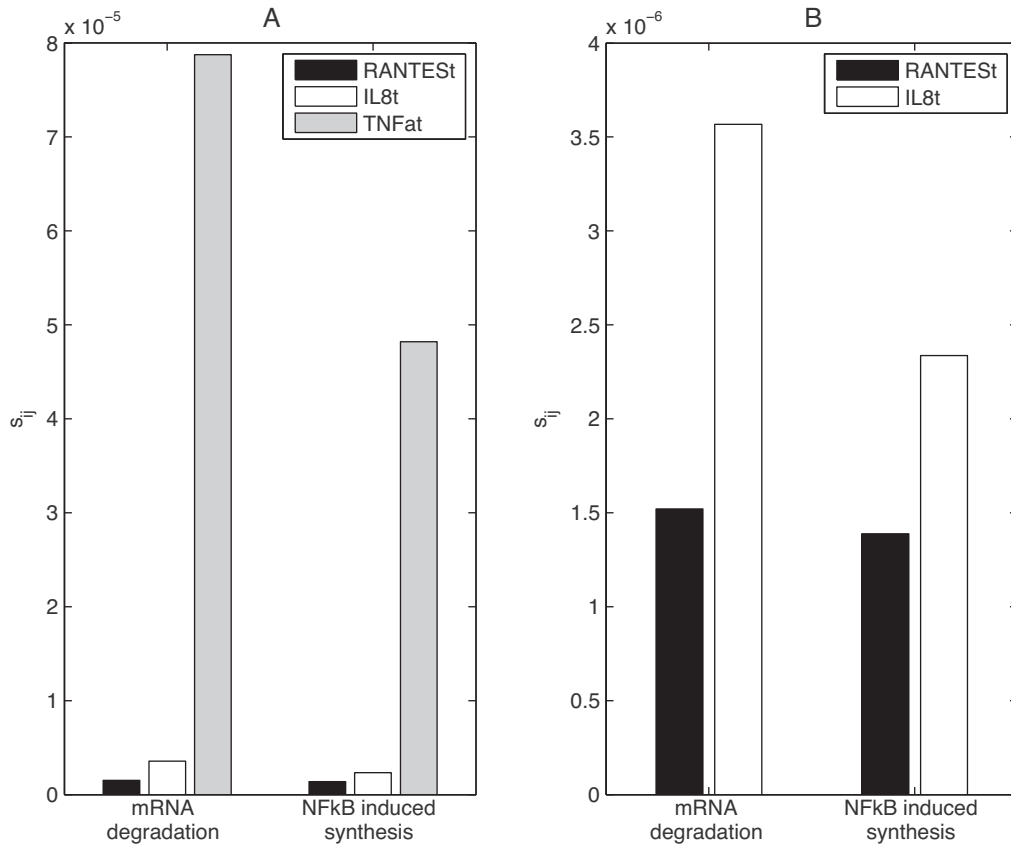


**Fig. 3.** Time independent sensitivities of the model parameters. Time independent sensitivities of the model parameters for degradation and synthesis of the cytokine mRNA expression levels with parameter increase or decrease of 40%. Model predictions with the estimated parameters were compared with model predictions of parameters increased or decreased by 40% and time independent sensitivity calculated. (A) *TNF $\alpha$*  shows the highest sensitivity of the three cytokines. *TNF $\alpha$*  is more sensitive to changes in parameters for degradation than NFkB induced synthesis. (B) The expression of *IL8* shows a higher sensitivity to degradation than to NFkB induced synthesis of mRNA, while in *RANTES* changes in either parameter have a similar influence on the expression levels.

### 3.3. Sensitivity analysis

#### 3.3.1. Sensitivity for initial species values

Sensitivities are calculated using time independent sensitivity as described in Section 4.3.2 (Eq. (12)). Initial species values and parameters that influenced the mRNA concentration over the 360 min simulation of the integrated model are ranked to identify the highest sensitivity (Supplement Table S1). The cytokines *RANTES*, *IL8*, *TNF $\alpha$*  are predominantly sensitive to the changes in the initial species values of I $\kappa$ B $\alpha$ /IKK $\beta$ . The sensitivity for *TNF $\alpha$*  increases towards the end of the simulation period (Supplement Fig. S4). Nuclear and cytoplasmic NFkB are also sensitive for initial species values of I $\kappa$ B $\alpha$ /IKK $\beta$ . However, while *RANTES* and *IL8* have similar top 4 rankings to nuclear NFkB (NFkB $_n$ ), *TNF $\alpha$*  follows cytoplasmic NFkB indicating a difference between the three cytokines and the need for the inclusion of the signaling pathway to elicit cytokine specific sensitivities.

#### 3.3.2. Sensitivity analysis for gene network regulation parameters

Time independent sensitivity (Section 4.3.2, Eq. (12)) for degradation parameters is higher than sensitivity for changes in NFkB transcription factor induced synthesis for each cytokine (Fig. 3).

Time dependent sensitivity (Section 4.3.1, Eq. (11)), the study of the effect of sensitivity over the simulation time, on the variation in the mRNA concentration indicates the largest variation in *TNF $\alpha$*  mRNA degradation parameter (Fig. 4).

A plot of the change in concentration over 360 min of simulation time for the changes of the synthesis and degradation

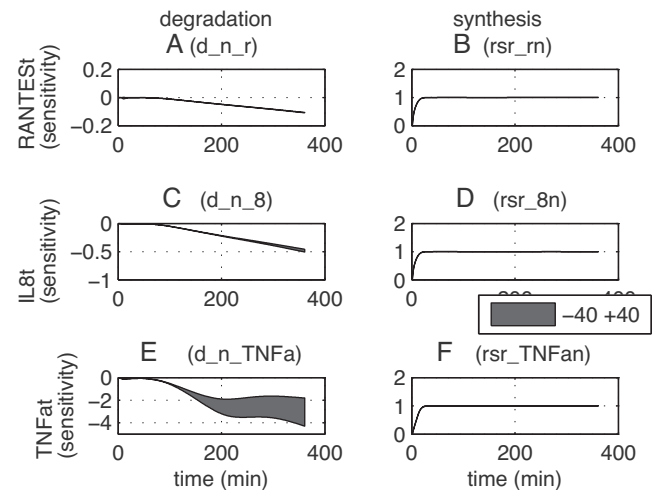


**Fig. 4.** Time dependent sensitivities of model parameters for degradation and synthesis of mRNA cytokine expression levels. Time dependent parameter sensitivities for degradation ( $d_n$ ) (A, C, and E) and synthesis ( $rsr_n$ ) (B, D, and F) of mRNA cytokine expression levels were calculated for parameter changes from -40% to +40% and the gradual change over the range is shown in the shaded areas. Sensitivity as result of changes in degradation parameters increases over model simulation time (A, C, and E), while sensitivity as result of change in synthesis parameters stays constant (B, D, and F). *TNF $\alpha$*  shows the largest variation in model sensitivity for the degradation parameter changes and the highest sensitivity values for the model (E).

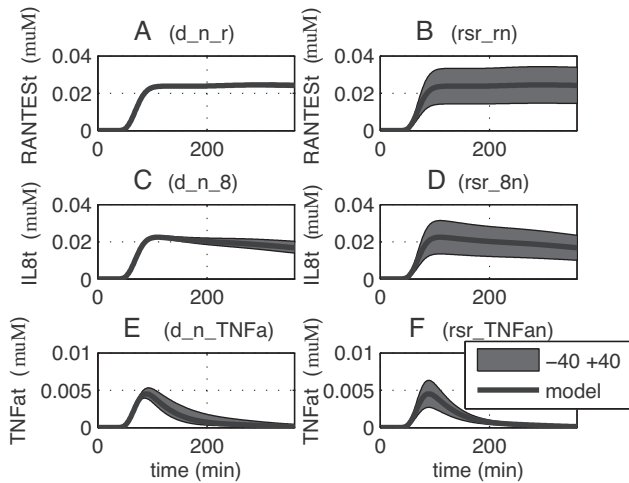


**Fig. 5.** Predicted expression levels for cytokine mRNA expression levels. Parameters for degradation (A, C, and E) and synthesis (B, D, and F) were changed from  $-40\%$  to  $+40\%$ . The gradual change over the range is shown in the shaded areas.

parameters clearly shows a changing influence over time on the cytokine mRNA concentration levels as a result of the parameter changes (Fig. 5).

*RANTES* degradation parameters have a small influence over this range on the concentration. The influence increases toward 360 min simulation predictions, while synthesis rates have larger but stable influence from 100 min onward (Fig. 5A and B). For the *IL8* mRNA cytokine, the changes in degradation rate increase their influence toward 360 min, while the changes in synthesis parameter show a stable influence from 100 min onward (Fig. 5C and D). *TNFalpha* synthesis and degradation parameters have a large influence at 90 min while the parameter changes have less influence on the changes in concentration levels at 360 min (Fig. 5E and F). This indicates a difference in sensitivity for synthesis and

degradation parameters for each cytokine over time, however, parameter changes do not change the trend.

### 3.3.3. Time independent sensitivity in signaling pathway

Time independent sensitivity analysis (Section 4.3.2) is used to rank the cytokine sensitivity for the large number of parameters in the signaling pathway (Fig. 6, Supplement Table S2).

The three most sensitive parameters identified in the time independent sensitivity analysis (Section 4.3.2, Eq. (12)) that influence the total mRNA concentration are analyzed in depth with time dependent sensitivity analysis.

Protein synthesis of  $I\kappa B\alpha$  (*rd\_a*), protein degradation of  $I\kappa B\alpha$  (*pd\_c\_3ain*) influencing NF $\kappa$ B and IKK concentration and  $I\kappa B\alpha$  mRNA degradation and synthesis are the major sensitivities in the model for *IL8* and *TNFalpha* mRNA expression (Supplement Table S2). *TNFalpha* shows the highest sensitivity to the parameter for protein degradation of  $I\kappa B\alpha$ IKKNF $\kappa$ B (*pd\_c\_3ain*). *TNFalpha* also showed a high sensitivity for the initial value of this complex. Earlier sensitivity studies of NF $\kappa$ B signaling as a result of *TNFalpha* challenge have identified parameters influencing these proteins most sensitive in the NF $\kappa$ B signaling process (Ihekwwaba et al., 2007; Yue et al., 2008). However, *RANTES* mRNA expression shows the largest sensitivity to NF $\kappa$ B import (*in\_n*) into the nucleus followed by protein degradation of  $I\kappa B\alpha$  in the cytoplasm and transport of  $I\kappa B\alpha$  into the nucleus. *RANTES* is a late gene that is activated only after prolonged exposure to NF $\kappa$ B in *TNFalpha* challenges (Ting et al., 2002). Therefore, finding the sensitivity to the parameter influencing nuclear NF $\kappa$ B import for mRNA expression of *RANTES* is in line with prior biological knowledge.

### 3.3.4. Time dependent sensitivity in signaling pathway

When the sensitivity (Section 4.3.1, Eq. (11)) of the identified parameters over time is plotted for the three species with the different parameters, a distinct difference for the time of the highest sensitivity between the cytokines *TNFalpha*, *RANTES* and *IL8* mRNA is noticed (Fig. 7).

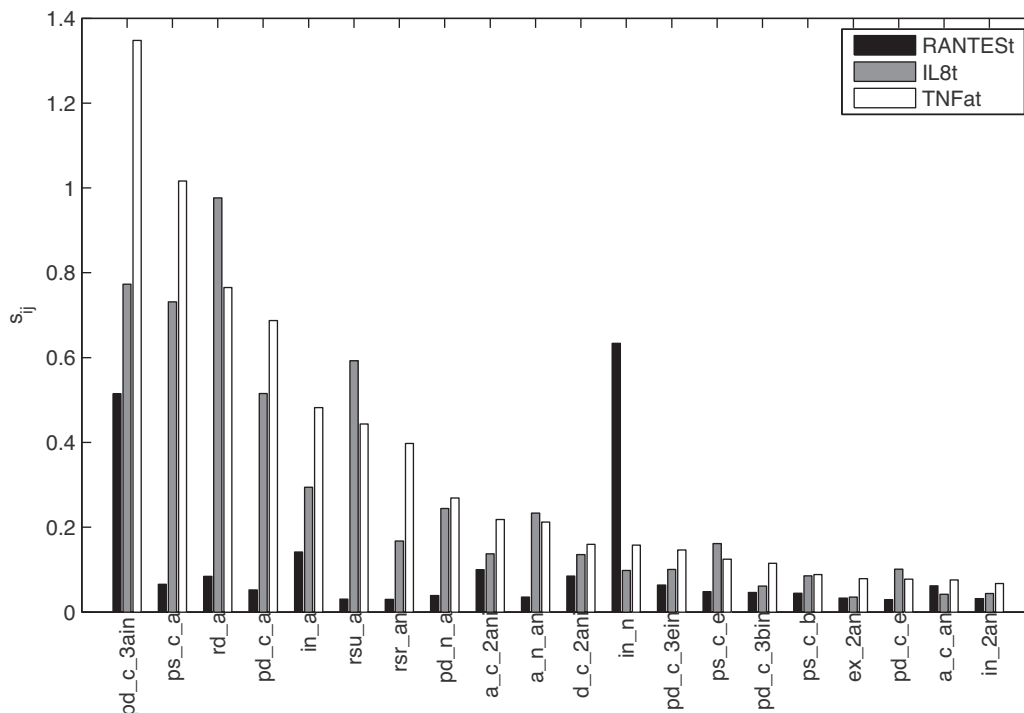


**Fig. 6.** Time independent sensitivities of the NF $\kappa$ B signaling parameters to the mRNA expression levels. Time independent sensitivities for the 40% variation in the top 20 parameters with the highest influence on the *RANTES*, *IL8* and *TNFalpha* mRNA expression levels.

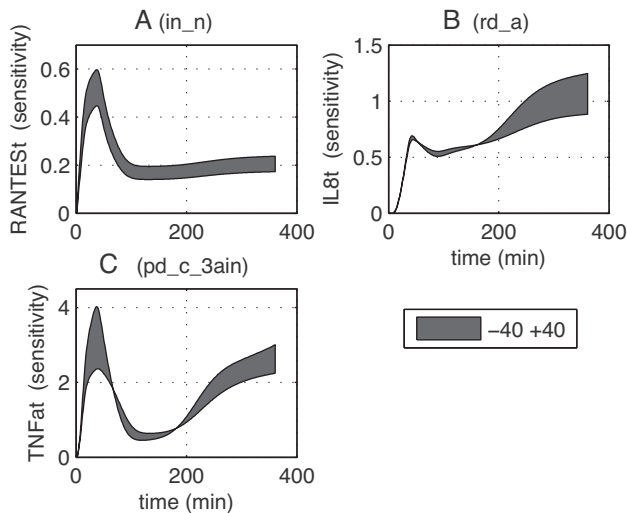


**Fig. 7.** Time dependent sensitivities over 360 min of simulation. The mRNA expression level variations for *RANTES*, *IL8* and *TNF $\alpha$*  for the parameters with the highest time independent sensitivity for each cytokine are shown. *RANTES* expression shows sensitivity for the transport of NF $\kappa$ B into the nucleus (*in\_n*). *IL8* is sensitive to the mRNA degradation of I $\kappa$ B $\alpha$  (*rd\_a*), specifically after 180 min and *TNF $\alpha$*  is sensitive to IKK mediated protein degradation (*pd\_c\_3ain*) in the initial phase of the model. In addition *TNF $\alpha$*  showed high sensitivity to the initial value of this protein.

*RANTES* is sensitive for the parameter change of parameter representing the transport of NF $\kappa$ B to the nucleus during the entire simulation time (Fig. 7A). This indicates sensitivity to parameter changes influencing exposure of NF $\kappa$ B over the entire simulation. *IL8* showed a change in sensitivity from 180 min onward (Fig. 7B) while *TNF $\alpha$*  showed sensitivity early in the simulation (Fig. 7C). It is clear that each cytokine expression levels is sensitive for changes in different components of the signaling pathway, something that would not have been possible with the study of the gene network in isolation. Neither would the parameter sensitivity in the signaling pathway of NF $\kappa$ B been able to identify the mechanism for the sensitivity in the cytokine expressions. This will become clearer with the study of parameter sensitivity of NF $\kappa$ B and the lack of the relationship between the ratio of nuclear and cytoplasmic NF $\kappa$ B and the cytokine expression level.

### 3.3.5. Comparison of signaling pathway parameter sensitivity for cytokines and nuclear and cytoplasmic NF $\kappa$ B

We compared the results of the time independent sensitivity ranking for the three cytokines with the time independent sensitivity ranking for nuclear and cytoplasmic NF $\kappa$ B (Supplement Table S2). The top three time independent sensitivity parameter rankings for nuclear NF $\kappa$ B is the same as the ranking for *IL8* mRNA. Cytoplasmic NF $\kappa$ B is similar to *TNF $\alpha$*  mRNA and the ranking for *RANTES* mRNA differs from both cytoplasmic and nuclear NF $\kappa$ B. While *IL8* and nuclear NF $\kappa$ B are sensitive to I $\kappa$ B $\alpha$  mRNA degradation rate changes, *TNF $\alpha$*  and cytoplasmic NF $\kappa$ B are sensitive to protein degradation of IKKNF $\kappa$ B/I $\kappa$ B $\alpha$ , releasing I $\kappa$ B $\alpha$ . Although the proteins located in the gene network and signaling pathway respectively, the sensitivity indicates a high sensitivity for the role of the negative feedback loop I $\kappa$ B $\alpha$  provides for these proteins. However, *RANTES* showed sensitivity for the import of NF $\kappa$ B into the nucleus. Interaction between I $\kappa$ B $\alpha$  and I $\kappa$ B $\epsilon$  has been indicated to be responsible for the translocation of NF $\kappa$ B from the cytoplasm to the nucleus. Between the three cytokines *RANTES* shows the highest ranking of parameters related to I $\kappa$ B $\epsilon$  (Supplement Table S2, *RANTES* 8th highest, with *IL8* 17th and *TNF $\alpha$*  13th). Indicating that *RANTES* is more sensitive to the

influence of the interaction between I $\kappa$ B $\alpha$  and I $\kappa$ B $\epsilon$  and the influence of I $\kappa$ B $\epsilon$  on the regulation of the negative feedback loop. There is therefore a distinct difference in the underlying mechanistic, originating in the signaling pathway, responsible for the variation in expression levels between the three cytokines. This cannot be explained by the nuclear or cytoplasmic NF $\kappa$ B sensitivity.

While one of the cytokines shows sensitivity similar to the nuclear NF $\kappa$ B and another to the cytoplasmic NF $\kappa$ B would it be possible to use the ratio of nuclear and cytoplasmic NF $\kappa$ B to identify the cytokine expression variation? The change in the ratio of NF $\kappa$ B in the cytoplasm and nucleus (NF $\kappa$ B:NF $\kappa$ Bn) was plotted over time for the range of  $-40\%$  to  $+40\%$  changes of the sensitive parameters identified above (Fig. 8).

*RANTES* shows sensitivity to change in translocation of NF $\kappa$ B from cytoplasm to the nucleus (*in\_n*) over the 360 min (Fig. 8A). A variation in the NF $\kappa$ B:NF $\kappa$ Bn ratio can also be seen with the changes of the parameter values for the translocation of NF $\kappa$ B to the nucleus (Fig. 8A) and the change in the concentration (Fig. 9A). In the first 50 min, the ratio varies with varying parameter values (Fig. 8A) and the sensitivity is high while there is no change in concentration (Fig. 9A).

Sensitivity then drops, however, the variation in sensitivity is the same while the variation in the ratio increases and then becomes stable and the variation in the concentration increases after 100 min and is stable for the remaining simulation period. However, there is no clear trend between the ratio and concentration of *RANTES* mRNA or the parameter sensitivity.

*IL8* shows sensitivity to the change in ratio after 120 min as a result of change in the parameter for RNA degradation of I $\kappa$ B $\alpha$  (*rd\_a*) (Fig. 8B). During this period, the ratio of NF $\kappa$ B between cytoplasm and nucleus changes significant but is stable while the sensitivity of *IL8* increases and therefore unlikely to be related.

*TNF $\alpha$*  mRNA expression is most sensitive in the early stages of the model simulation where there is a sharp decline in the NF $\kappa$ B

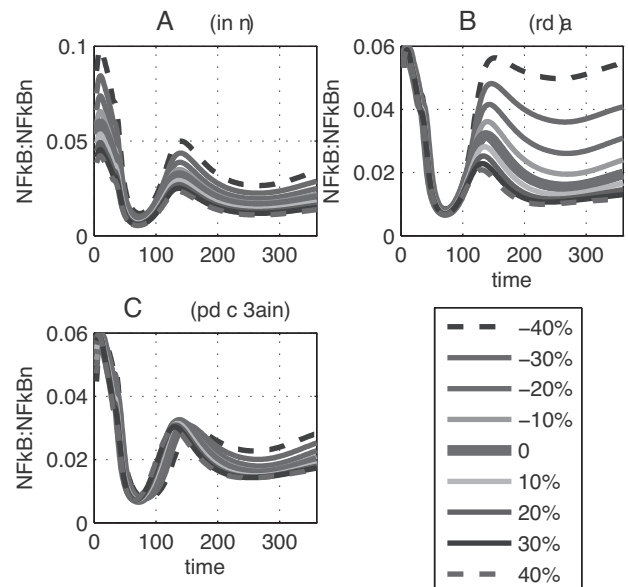


**Fig. 8.** Variation in NF $\kappa$ B cytoplasm:nucleus ratio for the highest ranked parameters. (A) NF $\kappa$ B ratio changes as result of parameter changes in transport of NF $\kappa$ B from the cytoplasm to the nucleus (*in\_n*) are consistent over the simulation time, which is similar to the changes in the *RANTES* mRNA concentration. (B) The NF $\kappa$ B ratio shows a change from 120 min onward, while after 180 min *IL8* mRNA shows a change in concentration with variation in mRNA degradation (*rd\_a*) of I $\kappa$ B $\alpha$ . (C) A relatively small change in the ratio is shown for parameter changes in IKK mediated protein degradation of I $\kappa$ B $\alpha$  (*pd\_c\_3ain*) indicated as the parameter with the highest rank in sensitivity analysis for *TNF $\alpha$*  mRNA concentration.

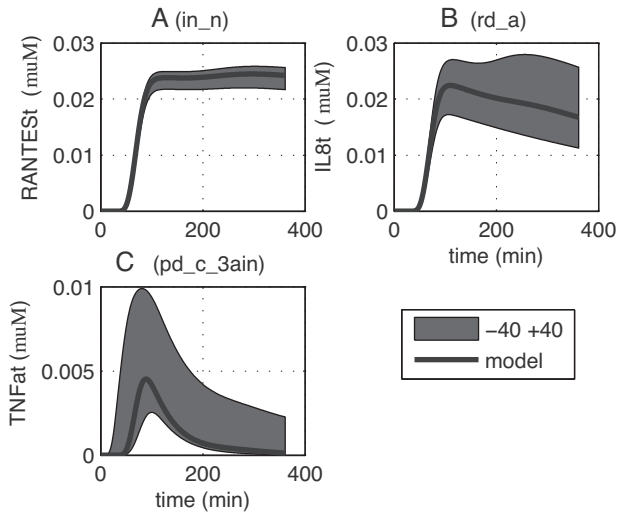


**Fig. 9.** mRNA concentration over 360 min of simulation with parameter changes (-40 to +40). The variation of the simulation over time for *RANTES*, *IL8* and *TNF $\alpha$*  for the parameters with the highest time independent sensitivity for each cytokine are shown. *RANTES* shows sensitivity for the transport of NF $\kappa$ B into the nucleus (*in\_n*), *IL8* is sensitive to the mRNA degradation of I $\kappa$ B $\alpha$  (*rd\_a*), specifically after 180 min and *TNF $\alpha$*  is sensitive to IKK mediated protein degradation (*pd\_c\_3ain*) in the initial phase of the model. In addition *TNF $\alpha$*  showed high sensitivity to the initial value of this protein.

ratio between cytoplasm and nucleus (Fig. 8C). However, there is no variation in the NF $\kappa$ B:NF $\kappa$ Bn ratio as a result of the parameter change and it is therefore unlikely to cause of the sensitivity.

It is therefore clear that neither the sensitivity of NF $\kappa$ B nor the NF $\kappa$ B:NF $\kappa$ Bn ratio can be used to explain the mechanism of the regulation or predict the cytokine expression levels. This indicates that the signaling pathway and the gene network need to be studied together to elicit the effect of intervention on the variation in cytokine mRNA expression. In addition, the effect of intervention, such as knocking out a signaling protein, need to be studied for each cytokine and the change in expression of one cytokine cannot be used to predict the others.

### 3.4. In silico knockout experiments

Some pharmaceutical products knock out the component in the signaling pathway rather than changing the rate of production or degradation. Prior *in silico* simulations of the integrated model can reduce the number of biological targets to investigate because biological networks often show a degree of redundancy. Several examples exist where the manipulation of one enzyme does not lead to the desired effect because of the redundancy in the system (van Someren et al., 2002). Inhibition of IKK $\beta$  was considered as a likely anti-inflammatory therapy (Greten et al., 2007). However, further studies revealed that IKK $\beta$  inhibition increased LPS susceptibility caused by IKK $\beta$ /NF $\kappa$ B dependent signaling of the negative feedback function of the NF $\kappa$ B induced cytokines (Park et al., 2005).

Investigation of the model sensitivity revealed that the highest ranked parameters influence the components NF $\kappa$ B and I $\kappa$ B $\alpha$ . To a lesser extent, the model is sensitive to parameter changes influencing the concentrations of I $\kappa$ B $\epsilon$  and I $\kappa$ B $\beta$  (Fig. 6). We thus investigated the effect of knockouts on the cytokine expression with *in silico* simulations in the integrated model.

#### 3.4.1. NF $\kappa$ B knockout simulation

Blocking NF $\kappa$ B is often suggested as a treatment in infections but has been shown to lead to sepsis (Liew et al., 2005). *In silico* simulation of the knockout of NF $\kappa$ B reduced the concentration of I $\kappa$ B $\alpha$  and I $\kappa$ B $\epsilon$  (Fig. 10D and E), while it increased the concentration of I $\kappa$ B $\beta$  (Fig. 10F).

Gene activation of I $\kappa$ B $\alpha$  and I $\kappa$ B $\epsilon$  is NF $\kappa$ B dependent. *RANTES*, *IL8* and *TNF $\alpha$*  show an immediate and sustained sharp decrease to 0 over the simulation period with NF $\kappa$ B knockout (Fig. 10C–E), which is to be expected.

Because we study the combined signaling and gene network regulation we can investigate the effects of varying other signaling proteins to vary, rather than block, NF $\kappa$ B level in the cytoplasm and nucleus and investigate redundancy.

#### 3.4.2. I $\kappa$ B $\alpha$ knockout simulation

*In silico* simulation of the protein I $\kappa$ B $\alpha$  or the I $\kappa$ B $\alpha$  mRNA knockout models show a substantial increase of mRNA levels of

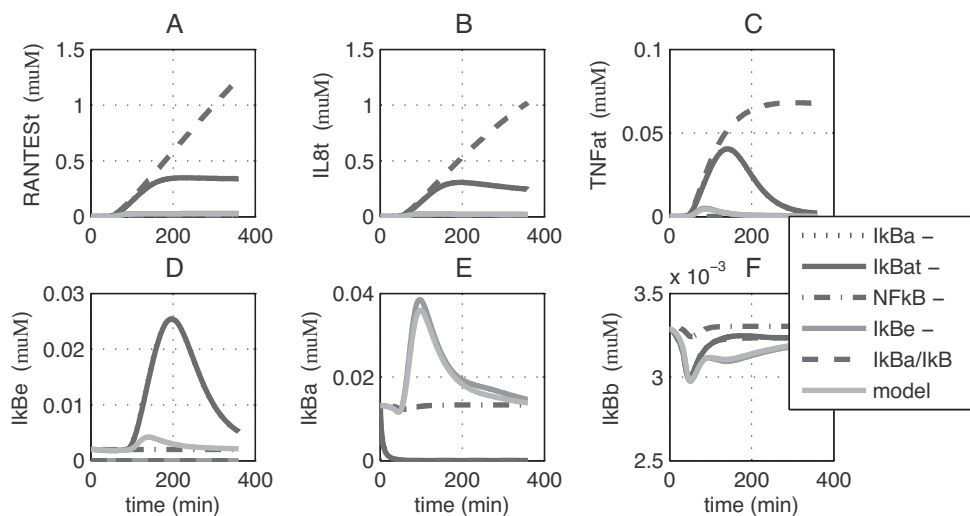


**Fig. 10.** Simulations of the model with I $\kappa$ B $\alpha$ , I $\kappa$ B $\alpha$  mRNA, NF $\kappa$ B, I $\kappa$ B $\epsilon$ , and the double knockout I $\kappa$ B $\alpha$ /I $\kappa$ B $\epsilon$ . Knockout models were generated from the wild type model by setting the initial value and the rate of expression to zero. (A and B) *RANTES* and *IL8* expression levels for the knockout models showed attenuation of the I $\kappa$ B $\alpha$ /I $\kappa$ B $\epsilon$  double knockout and raised levels for I $\kappa$ B $\alpha$  knockouts, while NF $\kappa$ B knockouts reduced the levels. (C) *TNF $\alpha$*  expression is raised with I $\kappa$ B $\alpha$ /I $\kappa$ B $\epsilon$  knockouts but returns to a stable level, while I $\kappa$ B $\alpha$  knockouts are raised but return to wild type level at 360 min and NF $\kappa$ B knockouts reduces the expression levels. (D) I $\kappa$ B $\epsilon$  levels are raised by I $\kappa$ B $\alpha$  and I $\kappa$ B $\epsilon$  knockouts but return to wild type level at 360 min of simulation. (E) I $\kappa$ B $\alpha$  levels were raised by the knockouts apart from the I $\kappa$ B $\epsilon$  knockout. I $\kappa$ B $\epsilon$  does not influence the level of I $\kappa$ B $\beta$ . Some knock outs I $\kappa$ B $\alpha$ , I $\kappa$ B $\alpha$  mRNA result in the same effect and do not show separately in the figures.

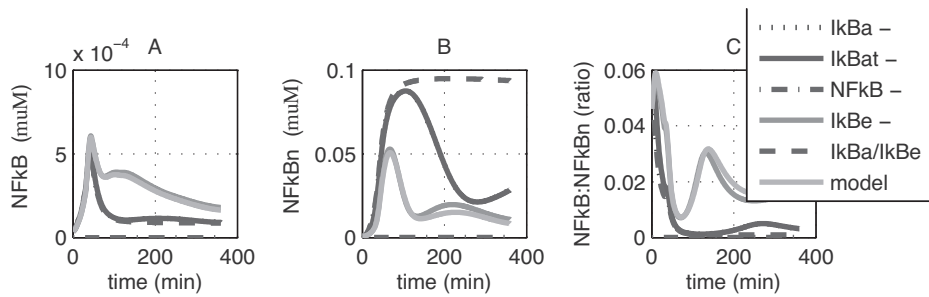


**Fig. 11.** *In silico* knockout simulations and the effect on NFκB. (A) NFκB (B) Nuclear NFκB (C) NFκB ratio.

*RANTES*, *IL8* and *TNFα* (Fig. 10A–C). The ratio of NFκB in the cytoplasm and nucleus changes. The NFκB in the cytoplasm is reduced as a result of the knockout of IκBα, while the nuclear NFκB increases (Fig. 12D and E).

This is expected since IκBα acts as a negative feedback loop. In the cytoplasm IκBα associates with NFκB preventing the movement of NFκB from the cytoplasm to the nucleus. Reduction of IκBα therefore increases the movement of NFκB to the nucleus where cytokine expression is initiated (Fig. 1).

Both *RANTES* and *IL8* show a prolonged increase in mRNA expression levels while the cytokine *TNFα* increases with a higher peak but reduces quickly to the wild type (WT) value when the NFκB reduces (Fig. 12A–C). The model therefore indicates a difference in kinetic response to the IκBα knockout between *RANTES*, *IL8* and *TNFα* mRNA. Due to the difference in magnitude in the degradation parameters between *RANTES* and *IL8* and *TNFα* this can be expected and is similar to earlier findings in the sensitivity analysis. The above sensitivity analysis (Section 3.3) identified different sensitivities for parameter changes for the individual cytokines. These parameters have different effects on the NFκB levels at different times and a different effect on the individual cytokines is to be expected. However, the mechanism is more complex and not influenced by IκBα alone. In addition to change in IκBα levels in the knockout simulation, the IKK concentration increases (Fig. 12F).

Increased concentration of IKK results in greater degradation of IκBα. The increased degradation then increases concentration of NFκB in the cytoplasm free to trans-locate to the nucleus. Although the reduction of NFκB in the nucleus shows a reduction of *TNFα* it does not explain the expression levels of *RANTES* or *IL8*.

The ratio of NFκB between cytoplasm and nucleus is more stable with the IκBα knockout explaining sustained gene expression of *RANTES* and *IL8* but not *TNFα*, neither does it explain the difference in the return to the wild type for *TNFα*. Looking at the NFκB ratio between cytoplasm and nucleus (Fig. 11C), the IκBα knockout reduces the ratio, stabilizing after 70 min with increased concentration of NFκB in the nucleus and reduced concentration of NFκB in the cytoplasm. This confirms that the ratio of NFκB between cytoplasm and nucleus cannot be used to predict cytokine levels and shows a level of redundancy in the model. However it shows that the manipulation of components in the signaling pathway, other than NFκB, can be used to manipulate distinctly different outcomes for the individual cytokines.

### 3.4.3. Multiple knockout simulations

The parameter sensitivity analysis did not indicate high sensitivity for the parameters influencing IκBε and IκBβ, however, knockout simulations show that the cytokine expression can be manipulated through multiple knockouts attenuating the effect of the IκBα knockout. *In silico* simulation of the IκBε and IκBβ

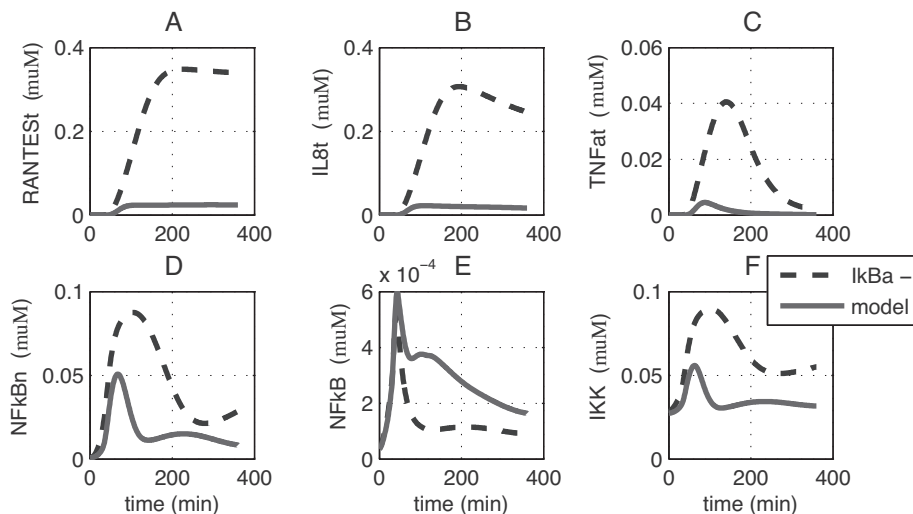


**Fig. 12.** Simulations of IκBα knockout and the effect on the different species. (A and B) *RANTES* and *IL8* do not return to the model values, while *TNFα* (C) does return to the model values. While nuclear NFκB (D) is higher than the model value, cellular NFκB (E) is lower than the model value. IKK (F) is increased and stays at increased level.

knockout models show almost no change of mRNA levels of *RANTES*, *IL8* and *TNF $\alpha$*  (Fig. 10A–C). The knockouts increase the  $\text{I}\kappa\text{B}\alpha$  concentration raising the peak minimally, returning back to the WT model values. NF $\kappa\text{B}$  in the cytoplasm and nucleus are marginally affected by the knockouts.

Simulating a double knockout of  $\text{I}\kappa\text{B}\alpha$  and  $\text{I}\kappa\text{B}\beta$  is not different from an  $\text{I}\kappa\text{B}\alpha$  knockout. However, a double knockout of  $\text{I}\kappa\text{B}\alpha$  and  $\text{I}\kappa\text{B}\epsilon$  attenuate the increase of NF $\kappa\text{B}$  in the nucleus but only marginally in the cytoplasm. The increase of NF $\kappa\text{B}$  in the nucleus results in a sustained elevation of *RANTES*, *IL8* and *TNF $\alpha$*  expression (Fig. 10A–C). The cytokine *TNF $\alpha$*  stabilizes, while the *IL8* and *RANTES* sustain increase. The knockout of the two negative feedback loops,  $\text{I}\kappa\text{B}\alpha$  and  $\text{I}\kappa\text{B}\epsilon$ , lead to an increase in the concentrations of nuclear NF $\kappa\text{B}$  that attenuate during the simulation period (Fig. 11B). There is no difference between  $\text{I}\kappa\text{B}\alpha$  knockout and  $\text{I}\kappa\text{B}\alpha\text{I}\kappa\text{B}\epsilon$  knockout with respect to NF $\kappa\text{B}$  in the cytoplasm, both reduce NF $\kappa\text{B}$ . The inhibitory role of  $\text{I}\kappa\text{B}\alpha$  and  $\text{I}\kappa\text{B}\epsilon$  in the form of negative feedback loops for the DNA-binding activity of NF $\kappa\text{B}$  of the TLR activated  $\text{I}\kappa\text{B}$ s as result of *TNF $\alpha$*  stimulation has been described earlier (Hoffmann et al., 2006).  $\text{I}\kappa\text{B}\alpha$  provides a negative feedback loop and is responsible for the post inductional down regulation of NF $\kappa\text{B}$  activation. The delayed  $\text{I}\kappa\text{B}\epsilon$  function is in an anti-phase to  $\text{I}\kappa\text{B}\alpha$ . It is proposed that the anti-phase regulation of  $\text{I}\kappa\text{B}\epsilon$  stabilizes the NF $\kappa\text{B}$  activity without reducing the ability to terminate NF $\kappa\text{B}$  activation after the removal of the stimulus (Hoffmann et al., 2006). The two kinases,  $\text{I}\kappa\text{B}\alpha$  and  $\text{I}\kappa\text{B}\epsilon$ , work in tandem to rapidly repress NF $\kappa\text{B}$  translocation after *TNF $\alpha$*  stimulation. A similar effect as result of *E. coli* stimulation is seen in this study. Pharmaceutical targets knocking out  $\text{I}\kappa\text{B}\alpha$  and  $\text{I}\kappa\text{B}\epsilon$  would therefore not achieve a reduction in cytokine levels but an increase.

### 3.5. Robustness in cytokine expression levels

We conducted several simulation experiments to investigate the effect of the change of the bacterial load, the model input, on the gene expression. We used the simulation output for robustness analysis to identify the source, in both the signaling and gene network, for the change in gene expression. Bacterial loads vary in mastitis due to milking. The model input, expressed in the function *ikkm* (Fig. 13), represent IKK profiles and simulate external perturbations e.g., bacterial loads. If IKK is knocked out no immune response will be evoked and the bacterial infection will continue to increase.

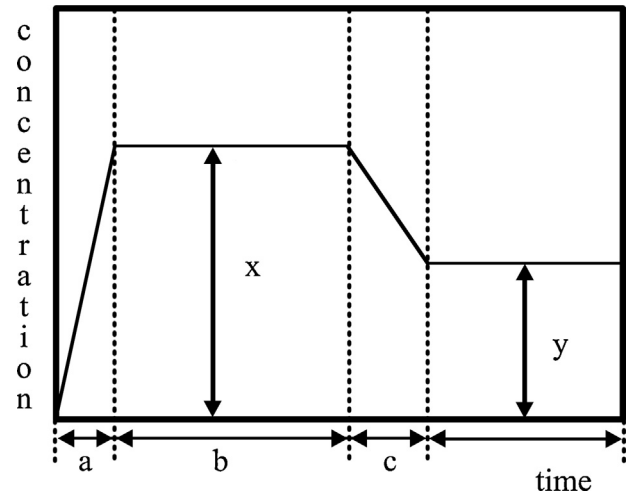


**Fig. 13.** IKK input profiles. A set of input profiles was generated varying the time of the rising, first plateau and falling phase ( $a$ – $c$ ) and the concentration in the first and second plateau ( $x$  and  $y$  with  $x > y$ ).

Rather than knocking out IKK it is therefore more informative to vary the IKK profiles (Fig. 13). Previously, simulations with varying IKK time profiles through variation in the *ikkm* function had identified 36 distinct nuclear NF $\kappa\text{B}$  time profiles (Werner et al., 2005). Nuclear NF $\kappa\text{B}$  is believed to be responsible for the cytokine expression level (Hayden et al., 2006) however, our sensitivity analysis showed that variation of NF $\kappa\text{B}$  does not influence the cytokines uniformly and is unique for each cytokine (Section 3.3). We therefore investigated the effect of the distinct nuclear NF $\kappa\text{B}$  time profiles on the cytokine expression levels with robustness analysis. Our simulation ran for 360 min. Increasing the range of values for the times ( $a$ – $c$  in Fig. 13) or concentration levels ( $x$  and  $y$  in Fig. 13) creating more than 2500 different input profiles did not increase the coverage of the input space or the number of different nuclear NF $\kappa\text{B}$  time profiles. Thus we chose one time profile from each cluster (Table 2) to simulate distinctly different external perturbations. We then clustered the cytokine profiles, using *k*-means clustering in MATLAB (Figs. 14 and 15).

The *in silico* simulations identified different correlations between the nuclear NF $\kappa\text{B}$  profiles and the cytokine *IL8* and *RANTES* and *TNF $\alpha$*  expression levels. In addition, the highest correlation between the cytokine concentration at 360 min and the

**Table 2**  
IKK input profiles generating 36 different nuclear NF $\kappa\text{B}$  time profiles ( $a$  = rising phase,  $b$  = first plateau,  $c$  = falling phase,  $x$  = concentration first plateau,  $y$  = concentration second plateau in Fig. 13).

	$a$ (min)	$b$ (min)	$c$ (min)	$x$ ( $\mu\text{M}$ )	$y$ ( $\mu\text{M}$ )		$a$ (min)	$b$ (min)	$c$ (min)	$x$ ( $\mu\text{M}$ )	$y$ ( $\mu\text{M}$ )
1	60	5	120	0.34	0.01	19	60	5	5	0.34	0.12
2	60	5	5	0.34	0.01	20	0	5	120	0.12	0.04
3	0	5	60	0.12	0.04	21	60	5	5	1.01	0.34
4	60	120	5	0.34	0.01	22	120	5	60	0.34	0.12
5	0	5	240	0.34	0.01	23	0	5	60	0.12	0.01
6	120	5	5	0.34	0.34	24	60	5	5	1.01	1.01
7	120	5	5	1.01	1.01	25	0	5	60	0.34	0.01
8	0	5	5	0.12	0.12	26	60	30	60	1.01	0.01
9	0	5	5	1.01	1.01	27	60	5	5	1.01	0.12
10	60	5	120	1.01	0.34	28	60	5	5	1.01	0.01
11	0	5	240	0.04	0.01	29	60	5	5	0.12	0.12
12	60	5	120	1.01	0.01	30	120	15	5	0.34	0.12
13	60	5	60	0.12	0.01	31	120	5	5	0.12	0.01
14	60	30	60	1.01	0.34	32	60	60	60	1.01	0.01
15	0	5	5	0.34	0.34	33	0	5	60	0.34	0.12
16	0	5	5	0.04	0.04	34	60	5	120	0.34	0.12
17	60	5	5	0.34	0.34	35	120	5	5	0.12	0.12
18	120	5	60	1.01	0.34	36	0	60	120	0.34	0.01

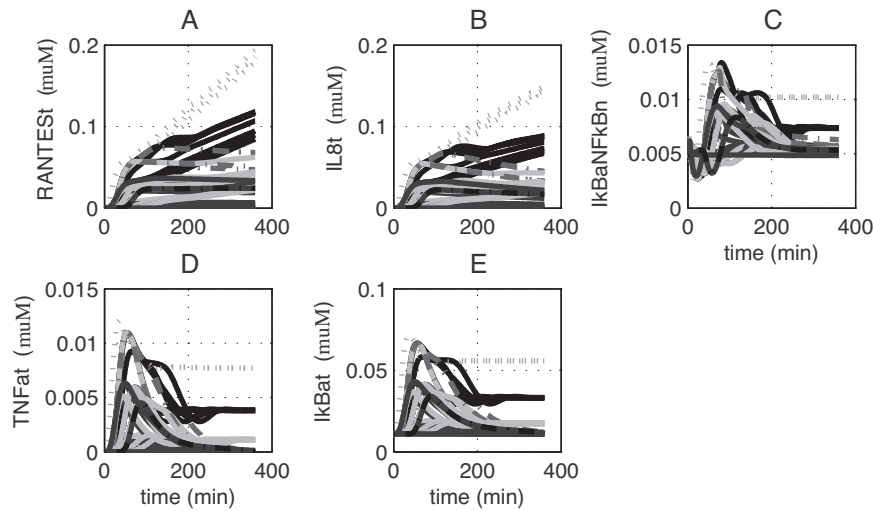


**Fig. 14.** Robustness in the gene network simulations with simulations clustered for nuclear  $I\kappa B\alpha NF\kappa B$  (A–C) and  $I\kappa B\alpha$  mRNA (E). (A) *RANTES* mRNA and (B) *IL8* mRNA showed the highest correlation ( $r=0.96$  and  $0.97$ ,  $p < 0.05$ ) with nuclear  $I\kappa B\alpha NF\kappa B$  in the gene network. (D) *TNF\alpha* mRNA showed the highest correlation with (E)  $I\kappa B\alpha$  mRNA ( $r=0.99$ ,  $p < 0.05$ ).

model species was not with nuclear or cytoplasmic  $NF\kappa B$  for any of the cytokines but with other species in the signaling pathway.

### 3.5.1. Robustness in gene network regulation

In the gene network, *RANTES* and *IL8* showed the highest correlation with nuclear  $I\kappa B\alpha NF\kappa B$  ( $r=0.96$  and  $0.97$ ,  $p < 0.05$ ), while *TNF\alpha* showed the highest correlation with  $I\kappa B\alpha$  mRNA ( $r=0.99$ ,  $p < 0.05$ ). The correlation with nuclear  $NF\kappa B$  was distinctly lower ( $r=0.80$  and  $0.82$ ,  $p < 0.05$ , Table 3).

Clustering the cytokine profiles and plotting the result together with the nuclear  $I\kappa B\alpha NF\kappa B$  (Fig. 14) shows a distinct difference between *RANTES* and *IL8* and *TNF\alpha*. While *TNF\alpha* will return to a stable state, *RANTES* and *IL8* will either continue to increase, for those clusters with a value higher than the original model, or decrease if the value is lower or equal than the model value and therefore depending on the cluster.

### 3.5.2. Robustness in signaling pathway

In the signaling pathway  $I\kappa B\epsilon$  showed the highest correlation with *RANTES* and *IL8* ( $r=0.95$  and  $0.97$ ,  $p < 0.05$ ), while  $I\kappa B\alpha$  showed the highest correlation with *TNF\alpha* ( $r=0.99$ ,  $p < 0.05$ ) (Fig. 15).

The correlation with cytoplasmic  $NF\kappa B$  was distinctly lower ( $r=0.88$  and  $0.91$ ,  $p < 0.05$ , Table 4).

The results indicates the need for a combined signaling and gene network regulation model because the underlying correlation with the  $I\kappa B\epsilon$  and  $I\kappa B\alpha$  variables would not have been identified with a gene network regulation model alone.

No relationship between the time of the *IL8* mRNA expression peak and nuclear  $NF\kappa B$  or any other components could be found. In milk samples, a higher bacterial load increased the *IL8* concentration and the time of the peak was earlier than with the lower bacterial load (Vangroenweghe et al., 2004).

Because we looked at the integrated model of the signaling pathway and gene network regulation we can also speculate on additional mechanisms. With our sensitivity analysis of gene network regulation for the cytokines we compared the relative sensitivity of synthesis and degradation parameter changes (Fig. 4E and F) with the change in concentration values for *TNF\alpha* mRNA expression (Fig. 5E and F). The sensitivity for parameter values increased, the concentration returned to the model levels, especially for variation in synthesis parameters at 360 min. It can be speculated that the robustness for variation in the synthesis

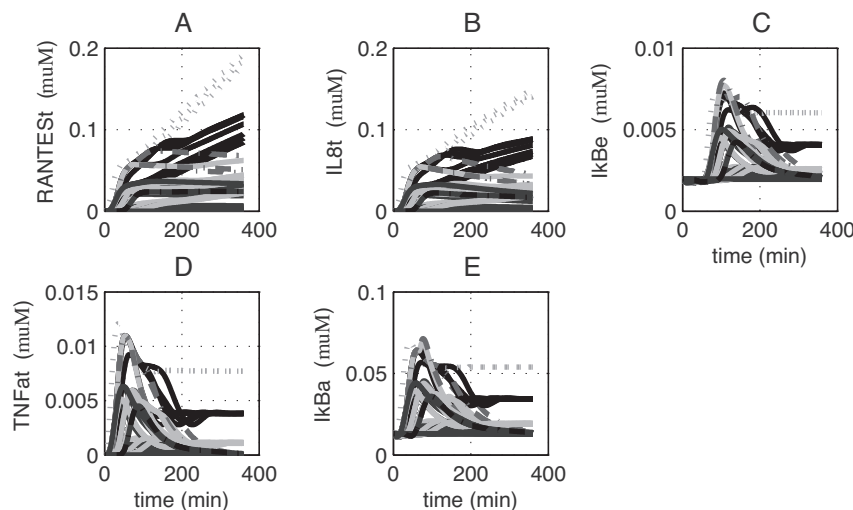


**Fig. 15.** Robustness in the signaling pathway simulations with simulations clustered for nuclear  $I\kappa B\epsilon$  (A–C) and  $I\kappa B\alpha$  (E). (A) *RANTES* mRNA and (B) *IL8* mRNA showed the highest correlation ( $r=0.95$  and  $0.97$ ,  $p < 0.05$ ) with  $I\kappa B\epsilon$  (C) in the signaling pathway. (D) *TNF\alpha* mRNA showed the highest correlation with (E)  $I\kappa B\alpha$  ( $r=0.99$ ,  $p < 0.05$ ).

**Table 3**

The highest correlation ( $p < 0.05$ ) between the change cytokine concentration and gene network regulation (IkB $\alpha$ , IkB $\alpha$ NFkB) components at 360 min. The correlation is calculated for the results of the 36 input variations simulating different NFkB profiles.

	<i>RANTES</i>	<i>IL8</i>	<i>TNF<math>\alpha</math></i>
IkB $\alpha$ NFkB	0.96	0.97	0.97
IkB $\alpha$ mRNA	0.94	0.96	0.99
NFkB	0.80	0.82	0.89

**Table 4**

The highest correlation ( $p < 0.05$ ) between the change cytokine concentration and the signaling (IkB $\alpha$ , IkB $\epsilon$ ) components at 360 min. The correlation is calculated for the results of the 36 input variations simulating different NFkB profiles.

	<i>RANTES</i>	<i>IL8</i>	<i>TNF<math>\alpha</math></i>
IkB $\alpha$	0.95	0.96	0.99
IkB $\epsilon$	0.95	0.97	0.99
NFkB	0.88	0.91	0.97

and degradation rates for *TNF $\alpha$*  mRNA in the mammary epithelial cells influences the robustness to variation in bacterial load at 360 min. It is thus possible that the robustness for synthesis and/or degradation parameter changes, rather than the robustness for change in NFkB regulation is the cause for robustness at 360 min observed in biological experiments. Changes in cytokine degradation rates as a result of disease have been seen earlier in other cells (Li and Bever, 2001) but need to be verified with biological experiments.

## 4. Methods

The experimental data used in this manuscript is described in the Supplementary information Section S1. In short, primary bovine mammary epithelial cells were taken from three cows and grown in culture. The cells were challenged with LPS simulating *E. coli* mammary infection. Gene expression, using Affymetrix bovine microarray time series, was measured and used for the model parameter estimation.

### 4.1. Mathematical modeling

The cytokine mRNA expression has been modeled in a modular way based on mass action kinetics using ODE. We based the signaling pathway model on a previously published model for TLR–IKK–NFkB signaling (Hoffmann et al., 2002; Werner et al., 2005). We implemented the ODE representing the mass balances of 24 components in the TLR–IKK–NFkB signaling in SBToolbox (Schmidt et al., 2006) in MATLAB (R2007a). The toolbox uses the MATLAB numerical differential equation solver, ode15s, to solve the equations. The *RANTES*, *IL8* and *TNF $\alpha$*  mRNA expression levels are represented by 3 additional ODEs. The integrated model consists of 27 ODEs and 89 reaction rates. Initial values were calculated by running the model with a basal input level (0.1  $\mu$ M) until no more changes in concentration could be detected. The MATLAB code is available upon request.

### 4.2. Parameter estimation

In order to verify the feasibility of the estimation of parameters for the differential equations with the measured data in our experiment, identifiability analysis is performed in SBtoolbox (Schmidt et al., 2006) with the method explained by Jacquez and Greif (1985). Parameter estimation and simulations for this model were performed using SBToolbox (Schmidt et al., 2006) in MATLAB (R2007a). Data processing of the experimental data prior to

parameter estimation is described in the Supplement (Section S2). In this paper a fast scatter search method is used (Egea et al., 2007; Rodriguez-Fernandez et al., 2006a). Fast scatter search is a combination of local and global optimization techniques, which aims to find the unknown parameters of the model that give the best goodness of fit to the experimental data.

We estimated the parameters and initial values to fit the converted mRNA expression levels of *RANTES*, *IL8* and *TNF $\alpha$* . Parameter estimations for models that include delay functions are slow and therefore we took the following steps: (i) the parameters for each cytokine were estimated in individual estimation runs, since identifiability indicates that the parameters between the cytokines were not correlated (see Supplement Section S2); (ii) the model was run with the estimated parameters for the individual cytokine and the model simulation results were compared with the experimental values for all three cytokines; (iii) iteratively the parameters were then estimated with the simulated values of the model that incorporated the estimated parameter values until no further optimization of the parameter values could be achieved with the fast scatter search (Rodriguez-Fernandez et al., 2006a,b); (iv) a final estimation round combining the parameters of the three ODEs was then performed with the fast scatter search algorithm as described in the methods until the value to satisfy the cost function was reached; and (v) the parameters were fined-tuned using manual tuning (Table 1, Section 3.1).

The parameter space is further explored in the sensitivity analysis as described in Section 3.3.

### 4.3. Sensitivity analysis

In local sensitivity analysis one parameter is changed at a time while the other parameter values are kept to their nominal values. The derivative vector,  $s_{ij}(t)$ , is calculated with Eqs. (10) and (11) to obtain a set of values for the finite parameter or initial value changes  $\delta$ , which allows us to compare the sensitive regions of the output of interest  $X$  for each parameter or initial value. The output of interest  $X$  can be any observable such as the concentration at time  $t$  of component  $X$  ( $[X]$ ) or a combination of the concentrations of several components ( $[X_1]$ ,  $[X_2]$ , . . .  $[X_n]$ ) at time  $t$ .  $\delta X$  stands for the incremental change in  $X$  due to the incremental change in the parameter  $\theta$  or initial value  $x(0)$ .

$$s_{ij}(t) = \frac{\delta(X_i(t))/X_i(t)}{\delta(\theta_j)/\theta_j} \quad (10)$$

$$s_{ij}(t) = \frac{\delta(X_i(t))/X_i(t)}{\delta(x_j(0))/x_j(0)} \quad (11)$$

#### 4.3.1. Time dependent sensitivity

The local normalized sensitivity of  $s_{ij}(t)$  is calculated for each time step  $t$  of the change in the  $i^{\text{th}}$  component  $X_i(t)$  with respect to the change in the  $j^{\text{th}}$  parameter  $\theta_j$  or initial value  $x_j(0)$  (Ihekawaba et al., 2004). Because of our interest in the fit of the model, the component  $X$  was chosen as the concentration of the cytokine mRNA at time  $t$  in the 360 min simulation period and evaluated for the synthesis and degradation parameter changes.

An uniform distribution of parameter values was created by changing the value of each parameter with incremental steps of 10% from the model parameter –40% to the model parameter +40% and the corresponding change in mRNA cytokine levels recorded. The value  $s_{ij}(t)$  will give a sensitivity index for each time step of the model simulation. However, time independent sensitivities would allow us to identify parameters with the

highest influence on the cytokine mRNA levels for the total simulation period.

#### 4.3.2. Time independent sensitivity

Integration of the sensitivities  $s_{ij}(t)$  gives a time-independent value that allows ranking of the individual sensitivities of each cytokine as a result of parameter changes Eq. (12).  $T$  is the final time point and absolute value of the integrand prevents positive and negative values cancelling to zero under the integral  $x_j(t)$  (Chen et al., 2009). The quantity  $S_{ij}$  measures the change in the concentration of the  $i^{\text{th}}$  component with respect to the  $j^{\text{th}}$  parameter normalized by  $T$  and therefore, captures variations in concentration level between parameter changes over time.

$$S_{ij} = \frac{1}{T} \int_0^T dt |s_{ij}(t)| \quad (12)$$

#### 4.4. In silico knock out simulations

The *in silico*  $\text{IkB}\alpha$ ,  $\text{NF}\kappa\text{B}$ ,  $\text{IkB}\epsilon$  and  $\text{IkB}\beta$  knockout models were generated from the wild type model by setting the initial value and the rate of expression of  $\text{IkB}\alpha$ ,  $\text{NF}\kappa\text{B}$ ,  $\text{IkB}\epsilon$  and  $\text{IkB}\beta$ , respectively to zero.

#### 4.5. Robustness analysis

In order to represent variation in bacterial load the input profile (Fig. 13) of the model is varied. Each profile contains a rising phase ( $a$  in Fig. 13), a first plateau ( $b$  in Fig. 13) and a second plateau ( $c$  in Fig. 13) with varying time levels ( $x$  and  $y$  in Fig. 13). To create a large set of diverse input profiles a computer program was developed. During a total simulation time of 360 min the duration of the rising phase was simulated for 0, 60, 120 and 240 min. The rise of the first plateau ( $x$ ) was simulated with 0.04, 0.12, 0.34 and 1.01  $\mu\text{M}$ . The duration of the first plateau ( $b$ ) was 0, 5, 15, 30, 60 or 120 min. The falling phase ( $c$ ) had duration of 0, 60, 120 or 240 min. The second plateau was equal or lower than the first plateau and varied between 0.01, 0.04, 0.12, 0.34 and 1.01  $\mu\text{M}$ .

The results of the simulations are clustered for nuclear cytokine concentrations at 360 min using the  $\kappa$ -means clustering algorithm implemented in Statistics Toolbox in MATLAB. Clusters are then compared with the components in the signaling pathway.

## 5. Conclusion

We set out to highlight the necessity for an integrated modeling approach of signaling pathway and gene networks. Gene expression, as a result of and external stimulus to cells, is investigated with a model combining the signaling pathway and gene network regulation. Signaling pathways and gene networks frequently have interdependent interactions that affect gene expression. Our integrated modular approach allows for investigation into a larger class of models without the need for extensive additional experiments, reducing cost and time.

We illustrated the value of the analysis of an integrated model with an example of the cytokines *RANTES*, *IL8* and *TNF $\alpha$*  mRNA expression regulation as a result of TLR–IKK–NF $\kappa$ B signaling and gene network regulation in *E. coli* challenge of mammary epithelial cells. It is known that *TNF $\alpha$* , *IL8* and *RANTES* are induced by the transcription factor NF $\kappa$ B as a result of TLR–IKK–NF $\kappa$ B signaling. NF $\kappa$ B has been long been recognized as the ‘master switch’ in regulating cytokine expression (Hayden et al., 2006).

Analysis of the model confirmed that the cytokine expression is not robust for variation to the NF $\kappa$ B time profile but the

mechanisms could not be identified with the gene network regulation model alone. However, the model identified signaling pathway components with higher sensitivity than NF $\kappa$ B in the regulation of the cytokine expression. In addition, time averaged sensitivity analysis of the integrated signaling and gene network regulation model identified sensitivity for different parameters and different times in the TLR–IKK–NF $\kappa$ B signaling cascade for each individual cytokine. Intuitively one would have expected variation of nuclear NF $\kappa$ B could explain the variation in each of the cytokines. Our simulations and analysis have proven otherwise.

The challenges of modeling biological systems lie in the decision of the appropriate abstraction level to focus on (Szallasi et al., 2006). In “Therefore all models are wrong . . . some more than others” Wolkenhauer and Ullah explains that it is a means of reducing complexity that motivates modeling (Wolkenhauer and Ullah, 2007). Integrating signaling pathway and gene network regulation increases complexity, however, with our model, we have shown that the increase is not prohibitive and the analysis identifies emerging properties underlying the differentiation of gene expression.

The model facilitates the fine-tuning of the individual cytokine expression levels through the manipulation of the components in the signaling cascade and the identification of the effects on the other cytokines. These effects and timing need to be taken into consideration when developing drugs or planning future experiments. As the model analysis has indicated, the optimum experimental time differs between the cytokines. In addition drugs targeting these parameters will have a different effect over time on the cytokines. As the predictions are based on *in silico* models, the validity of the results should be experimentally tested, however, this is beyond the scope of the current work.

## Acknowledgements

Nicoline Y. den Breems was funded by the Patrick Shannon Scholarship from LIC and the EU FP7 BIOMICS project (Grant No. 318202). Lan K. Nguyen was supported by funding provided by SFI (Grant No. 06/CE/B1129) and PRIMES (FP7-HEALTH-2011-278568) and University College Dublin’s Seed Funding program. We would like to thank Professor Hans-Martin Seyfert for the use of the microarray data.

## Appendix A. Supplementary data

Supplementary data associated with this article can be found, in the online version, at <http://dx.doi.org/10.1016/j.biosystems.2014.09.011>.

## References

- Akira, S., Uematsu, S., Takeuchi, O., 2006. Pathogen recognition and innate immunity. *Cell* 124 (4), 783–801.
- Bannerman, D.D., Paape, M.J., Lee, J.W., Zhao, X., Hope, J.C., Rainard, P., 2004. *Escherichia coli* and *Staphylococcus aureus* elicit differential innate immune responses following intramammary infection. *Clin. Diagn. Lab. Immunol.* 11 (3), 463–472.
- Bhalla, U.S., Iyengar, R., 1999. Emergent properties of networks of biological signaling pathways. *Science* 283 (5400), 381–387.
- Boulanger, D., Bureau, F., Melotte, D., Mainil, J., Lekeux, P., 2003. Increased nuclear factor kappaB activity in milk cells of mastitis-affected cows. *J. Dairy Sci.* 86 (4), 1259–1267.
- Bragt, M., Plat, J., Mensink, M., Schrauwen, P., Mensink, R., 2009. Anti-inflammatory effect of rosiglitazone is not reflected in expression of nuclear factor kappaB-related genes in peripheral blood mononuclear cells of patients with type 2 diabetes mellitus. *BMC Endocr. Disord.* 9 (1), 8.
- Brandman, O., Meyer, T., 2008. Feedback loops shape cellular signals in space and time. *Science* 322 (5900), 390–395.
- Chen, W.W., Schoeberl, B., Jasper, P.J., Niepel, M., Nielsen, U.B., Lauffenburger, D.A., Sorger, P.K., 2009. Input-output behavior of ErbB signaling pathways as revealed by a mass action model trained against dynamic data. *Mol. Syst. Biol.* 5, 239.

- Cheong, R., Hoffmann, A., Levchenko, A., 2008. Understanding nuclear factor kappaB signaling via mathematical modeling. *Mol. Syst. Biol.* 4, 192.
- Connelly, L., Barham, W., Pigg, R., Saint-Jean, L., Sherrill, T., Cheng, D.-S., Yull, F.E., 2010. Activation of nuclear factor kappa B in mammary epithelium promotes milk loss during mammary development and infection. *J. Cell. Physiol.* 222 (1), 73–81.
- Covert, M.W., Leung, T.H., Gaston, J.E., Baltimore, D., 2005. Achieving stability of lipopolysaccharide-induced nuclear factor kappaB activation. *Science* 309 (5742), 1854–1857.
- de Jong, H., Ropers, D., 2006. Qualitative approaches to the analysis of genetic regulatory networks. In: Szallasi, Z. (Ed.), *Systems Modeling in Cellular Biology*. MIT, Cambridge, USA, pp. 125–147.
- De Ketelaere, A., Goossens, K., Peelman, L., Burvenich, C., 2006. Technical note: validation of internal control genes for gene expression analysis in bovine polymorphonuclear leukocytes. *J. Dairy Sci.* 89 (10), 4066–4069.
- De Schepper, S., De Ketelaere, A., Bannerman, D.D., Paape, M.J., Peelman, L., Burvenich, C., 2008. The toll-like receptor-4 (TLR-4) pathway and its possible role in the pathogenesis of *Escherichia coli* mastitis in dairy cattle. *Vet. Res.* 39 (1), 5.
- Doyle, S.L., O'Neill, L.A., 2006. Toll-like receptors: from the discovery of nuclear factor kappaB to new insights into transcriptional regulations in innate immunity. *Biochem. Pharmacol.* 72 (9), 1102–1113.
- Egea, J., Rodríguez-Fernández, M., Banga, J., Martí, R., 2007. Scatter search for chemical and bio-process optimization. *J. Glob. Optim.* 37 (3), 481–503(423).
- Fraser, C.C., 2008. G Protein coupled receptor connectivity to nuclear factor kappaB in inflammation and cancer. *Int. Rev. Immunol.* 27 (5), 320–350.
- Goldstein, B., Faeder, J.R., Hlavacek, W.S., 2004. Mathematical and computational models of immune-receptor signalling. *Nat. Rev. Immunol.* 4 (6), 445–456.
- Greten, F.R., Arkan, M.C., Bollrath, J., Hsu, L.C., Goode, J., Miething, C., Karin, M., 2007. Nuclear factor kappaB is a negative regulator of IL-1beta secretion as revealed by genetic and pharmacological inhibition of IKKbeta. *Cell* 130 (5), 918–931.
- Griesbeck-Zilch, B., Meyer, H.H., Kuhn, C.H., Schwerin, M., Wellnitz, O., 2008. *Staphylococcus aureus* and *Escherichia coli* cause deviating expression profiles of cytokines and lactoferrin messenger ribonucleic acid in mammary epithelial cells. *J. Dairy Sci.* 91 (6), 2215–2224.
- Griesbeck-Zilch, B., Osman, M., Kuhn, C., Schwerin, M., Bruckmaier, R.H., Pfaffl, M.W., Wellnitz, O., 2009. Analysis of key molecules of the innate immune system in mammary epithelial cells isolated from marker-assisted and conventionally selected cattle. *J. Dairy Sci.* 92 (9), 4621–4633.
- Hayden, M.S., West, A.P., Ghosh, S., 2006. Nuclear factor kappaB and the immune response. *Oncogene* 25 (51), 6758–6780.
- Hoffmann, A., Baltimore, D., 2006. Circuitry of nuclear factor kappaB signaling. *Immunol. Rev.* 210, 171–186.
- Hoffmann, A., Levchenko, A., Scott, M.L., Baltimore, D., 2002. The IkappaB-nuclear factor kappaB signaling module: temporal control and selective gene activation. *Science* 298 (5596), 1241–1245.
- Hoffmann, A., Natoli, G., Ghosh, G., 2006. Transcriptional regulation via the nuclear factor kappaB signaling module. *Oncogene* 25 (51), 6706–6716.
- Hornberg, J.J., Bruggeman, F.J., Westerhoff, H.V., Lankelma, J., 2006. Cancer: a systems biology disease. *BioSystems* 83 (2–3), 81–90.
- Ihekwa, A.E., Broomhead, D.S., Grimley, R.L., Benson, N., Kell, D.B., 2004. Sensitivity analysis of parameters controlling oscillatory signalling in the nuclear factor kappaB pathway: the roles of IKK and IkappaBalpha. *Syst. Biol.* 1 (1), 93–103.
- Ihekwa, A.E.C., Wilkinson, S.J., Waithe, D., Broomhead, D.S., Li, P., Grimley, R.L., Benson, N., 2007. Bridging the gap between *in silico* and cell-based analysis of the nuclear factor kappaB signaling pathway by *in vitro* studies of IKK2. *FEBS J.* 274 (7), 1678–1690.
- Jacquez, J.A., Greif, P., 1985. Numerical parameter identifiability and estimability: integrating identifiability, estimability, and optimal sampling design. *Math. Biosci.* 77 (1–2), 201–227.
- John, G.C., Nduati, R.W., Mbori-Ngacha, D.A., Richardson, B.A., Panteleeff, D., Mwatha, A., Kreiss, J.K., 2001. Correlates of mother-to-child human immunodeficiency virus type 1 (HIV-1) transmission: association with maternal plasma HIV-1 RNA load, genital HIV-1 DNA shedding, and breast infections. *J. Infect. Dis.* 183 (2), 206–212.
- Kawai, T., Akira, S., 2006. TLR signaling. *Cell Death Diff.* 13 (5), 816–825.
- Kearns, J.D., Basak, S., Werner, S.L., Huang, C.S., Hoffmann, A., 2006. IkappaBepsilon provides negative feedback to control nuclear factor kappaB oscillations, signaling dynamics, and inflammatory gene expression. *J. Cell Biol.* 173 (5), 659–664.
- Kearns, J.D., Hoffmann, A., 2008. Integrating computational and biochemical studies to explore mechanisms in nuclear factor kappa B signaling. *J. Biol. Chem.* 284 (9), 5439–5443.
- Kell, D.B., 2005. Metabolics, machine learning and modelling: towards an understanding of the language of cells. *Biochem. Soc. Trans.* 33 (3), 520–524.
- Lahouassa, H., Moussay, E., Rainard, P., Riollet, C., 2007. Differential cytokine and chemokine responses of bovine mammary epithelial cells to *Staphylococcus aureus* and *Escherichia coli*. *Cytokine* 38 (1), 12–21.
- Li, Q.Q., Bever, C.T., 2001. Mechanisms underlying the synergistic effect of Th1 cytokines on RANTES chemokine production by human glial cells. *Int. J. Mol. Med.* 7 (2), 187–195.
- Liew, F.Y., Xu, D., Brint, E.K., O'Neill, L.A.J., 2005. Negative regulation of toll-like receptor-mediated immune responses. *Nat. Rev. Immunol.* 5 (6), 446–458.
- Ling, H., Samarasinghe, S., Kulasiri, D., 2013. Novel recurrent neural network for modelling biological networks: oscillatory p53 interaction dynamics. *BioSystems* 114 (3), 191–205.
- Lipniacki, T., Paszek, P., Brasier, A.R., Luxon, B., Kimmel, M., 2004. Mathematical model of nuclear factor kappaB regulatory module. *J. Theor. Biol.* 228 (2), 195–215.
- Lutzow, Y.C., Donaldson, L., Gray, C.P., Vuocolo, T., Pearson, R.D., Reverter, A., Tellam, R.L., 2008. Identification of immune genes and proteins involved in the response of bovine mammary tissue to *Staphylococcus aureus* infection. *BMC Vet. Res.* 4, 18.
- Nelson, D.E., Ihekwa, A.E.C., Elliott, M., Johnson, J.R., Gibney, C.A., Foreman, B.E., White, M.R.H., 2004. Oscillations in nuclear factor kappaB signaling control the dynamics of gene expression. *Science* 306 (5696), 704–708.
- Pareek, R., Wellnitz, O., Van Dorp, R., Burton, J., Kerr, D., 2005. Immunorelevant gene expression in LPS-challenged bovine mammary epithelial cells. *J. Appl. Genet.* 46 (2), 171–177.
- Park, J.M., Greten, F.R., Wong, A., Westrick, R.J., Arthur, J.S., Otsu, K., Karin, 2005. Signaling pathways and genes that inhibit pathogen-induced macrophage apoptosis – CREB and NF-kappaB as key regulators. *Immunity* 23 (3), 319–329.
- Petzl, W., Zerbe, H., Gunther, J., Yang, W., Seyfert, H.M., Nurnberg, G., Schuberth, H.J., 2008. *Escherichia coli*, but not *Staphylococcus aureus* triggers an early increased expression of factors contributing to the innate immune defense in the udder of the cow. *Vet. Res.* 39 (2), 18.
- Rainard, P., Riollet, C., 2006. Innate immunity of the bovine mammary gland. *Vet. Res.* 37 (3), 369–400.
- Rodriguez-Fernandez, M., Egea, J.A., Banga, J.R., 2006a. Novel metaheuristic for parameter estimation in nonlinear dynamic biological systems. *BMC Bioinform.* 7, 483.
- Rodriguez-Fernandez, M., Mendes, P., Banga, J.R., 2006b. A hybrid approach for efficient and robust parameter estimation in biochemical pathways. *BioSystems* 83 (2–3), 248–265.
- Schlitt, T., Brazha, A., 2007. Current approaches to gene regulatory network modelling. *BMC Bioinform.* 8 (Suppl. 6), S9.
- Schmidt, H., Jirstrand, M., 2006. Systems biology toolbox for MATLAB: a computational platform for research in systems biology. *Bioinformatics* 22 (4), 514–515.
- Sillitoe, K., Horton, C., Spiller, D.G., White, M.R.H., 2007. Single-cell time-lapse imaging of the dynamic control of nuclear factor kappa B signalling. *Biochem. Soc. Trans.* 35, 263–266.
- Strandberg, Y., Gray, C., Vuocolo, T., Donaldson, L., Broadway, M., Tellam, R., 2005. Lipopolysaccharide and lipoteichoic acid induce different innate immune responses in bovine mammary epithelial cells. *Cytokine* 31 (1), 72–86.
- Sung, M.H., Simon, R., 2004. *In silico* simulation of inhibitor drug effects on nuclear factor kappaB pathway dynamics. *Mol. Pharmacol.* 66 (1), 70–75.
- Suresh Babu, C.V., Joo Song, E., Yoo, Y.S., 2006. Modeling and simulation in signal transduction pathways: a systems biology approach. *Biochimie* 88 (3–4), 277–283.
- Szallasi, Z., Stelling, J., Periwai, V., 2006. *System Modeling in Cell Biology: From Concepts to Nuts and Bolts*. MIT Press, Cambridge, Massachusetts, USA.
- Tao, W., Mallard, B., 2007. Differentially expressed genes associated with *Staphylococcus aureus* mastitis of Canadian Holstein cows. *Vet. Immunol. Immunopathol.* 120 (3–4), 201–211.
- Thakar, J., Piliome, M., Kirimanjswara, G., Harvill, E.T., Albert, R., 2007. Modeling systems-level regulation of host immune responses. *PLoS Comput. Biol.* 3 (6), e109.
- Ting, A.Y., Endy, D., 2002. Signal transduction. Decoding nuclear factor kappaB signaling. *Science* 298 (5596), 1189–1190.
- van Someren, E.P., Wessels, L.F., Backer, E., Reinders, M.J., 2002. Genetic network modeling. *Pharmacogenomics* 3 (4), 507–525.
- Vanden Berghe, W., Ndlovu, M.N., Hoya-Arias, R., Dijsselbloem, N., Gerlo, S., Haegeman, G., 2006. Keeping up nuclear factor kappaB appearances: epigenetic control of immunity or inflammation-triggered epigenetics. *Biochem. Pharmacol.* 72 (9), 1114–1131.
- Vangroenweghe, F., Rainard, P., Paape, M., Duchateau, L., Burvenich, C., 2004. Increase of *Escherichia coli* inoculum doses induces faster innate immune response in primiparous cows. *J. Dairy Sci.* 87 (12), 4132–4144.
- Vera, J., Bachmann, J., Pfeifer, A.C., Becker, V., Hormiga, J.A., Torres Darias, N.V., Wolkenhauer, O., 2008. A systems biology approach to analyse amplification in the JAK2-STAT5 signalling pathway. *BMC Syst. Biol.* 2 (1), 38.
- Vera, J., Balsa-Canto, E., Wellstead, P., Banga, J.R., Wolkenhauer, O., 2007. Power-law models of signal transduction pathways. *Cell. Signal.* 19 (7), 1531–1541.
- Viatour, P., Merville, M.P., Bours, V., Chariot, A., 2005. Phosphorylation of nuclear factor kappaB and IkappaB proteins: implications in cancer and inflammation. *Trends Biochem. Sci.* 30 (1), 43–52.
- Wang, L.Y., Chen, C.T., Liu, W.H., Wang, Y.H., 2007. Recurrent neonatal group B streptococcal disease associated with infected breast milk. *Clin. Pediatr.* 46 (6), 547–549.
- Werner, S.L., Barken, D., Hoffmann, A., 2005. Stimulus specificity of gene expression programs determined by temporal control of IKK activity. *Science* 309 (5742), 1857–1861.
- Wolkenhauer, O., Ullah, M., 2007. All models are wrong, some more than others. In: Boogerd, F., Bruggeman, F.J., Hofmeyr, J.H.S., Westerhoff, H.V. (Eds.), *Systems Biology: Philosophical Foundations*. Elsevier Science, Amsterdam, the Netherlands, pp. 163–179.
- Wolkenhauer, O., Ullah, M., Wellstead, P., Cho, K.H., 2005. The dynamic systems approach to control and regulation of intracellular networks. *FEBS Lett.* 579 (8), 1846–1853.
- Xie, Z., Kulasiri, D., 2007. Modelling of circadian rhythms in *Drosophila* incorporating the interlocked PER/TIM and VRI/PDP1 feedback loops. *J. Theor. Biol.* 245 (2), 290–304.
- Yue, H., Brown, M., He, F., Jia, J., Kell, D.B., 2008. Sensitivity analysis and robust experimental design of a signal transduction pathway system. *Int. J. Chem. Kinet.* 40 (11), 730–741.